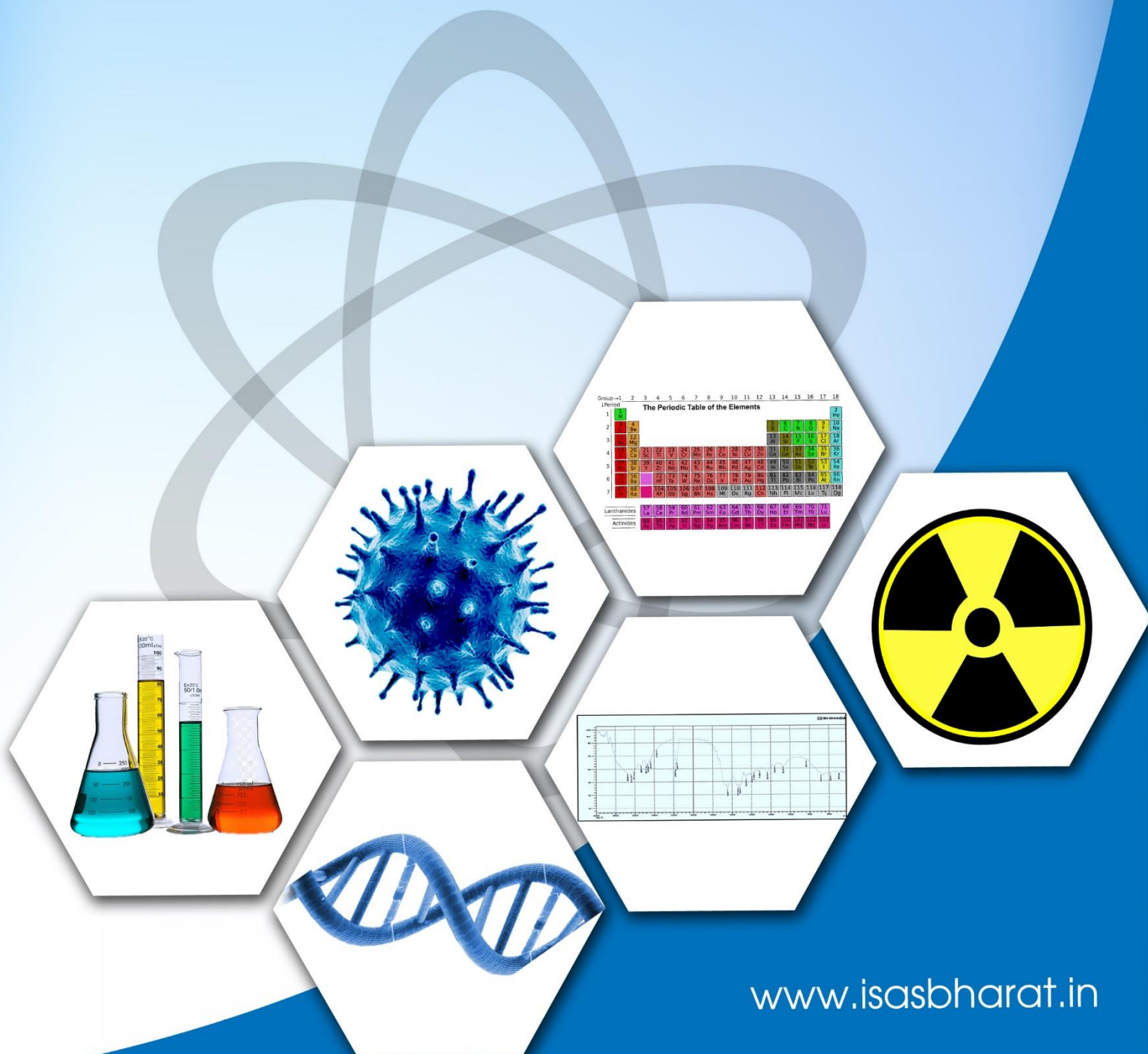




ISSN: 2583-5459
Volume 3 Issue 1
July, 2024

Journal of ISAS

An open access peer reviewed quarterly e-journal by
Indian Society of Analytical Scientists





Journal of ISAS

An open access peer reviewed quarterly e-journal published by Indian Society of Analytical Scientists

Published by: Indian Society of Analytical Scientists (ISAS)

Address: C/o REDS, BARC, Mumbai 400085

Email: isasjournal@isasbharat.in

President ISAS: Dr. Raghaw Saran

J. ISAS

Editorial Board

Editor in Chief

Dr. Nilima Rajurkar, Pune

Members

Dr. Vijayalaxmi C. Adya, Mumbai

Dr. A. K. Basu, Pune

Dr. Vinay Bhandari, Pune

Dr. Avinash Bharati, Nagpur

Dr. Anu Gopinath, Kochi

Dr. Ravin Jugade, Nagpur

Dr. Padmaja S. Vadodara

Dr. Pradeep Kumar, Mumbai

Dr. Prakash Samnani, Vadodara

Dr. Sridhar T. M , Chennai

Dr. S. K. Yadav, Vadodara

Dr. A. N. Garg, New Delhi

Advisory Board

Chairman

Dr. Raghaw Saran, Nagpur

Members

Dr. V. Sivanandan Achari, Kochi

Dr. V. Balaram, Hyderabad

Dr. J. Manjanna, Belgavi

Dr. V. R.Nair, Kollam

Dr. Amrit Prakash, Mumbai

Dr. S. Sriman Narayanan, Vellur

Dr. Shivaramu Prasanna, Bengaluru

Dr. K.P. Vijayalakshmi, Trivandrum

Dr. Mohammed Yusuff K.K., Kochi

Dr. Rajeev Raghavan, Trivandrum

Instruction to Authors

- The Manuscript should be typed in **MS word** (times new roman) with **1.5 spacings** and **font size 12**
- The **title** of the paper should be clear and concise(**font size 14 and bold**), the first letter of each noun and adjective in the title must be in capital letter. It will be followed by names of authors(initials followed by surname) with their affiliation (**font size 12**)
- Corresponding author should be indicated by * with email ID
- The text should be divided into following sections:
 - **Abstract : up to 300 words**
 - **Key words: 5-6**
 - **Introduction**
 - **Experimental**
 - **Results and Discussion**
 - **Conclusions**
 - **Acknowledgement**
- Figures and Tables should be before references with a caption **Figures:** Followed by **Tables:**
- **References**
 - Divisions within the section should be indicated as subheadings
 - The figures and tables should be numbered with Roman numerals and must be mentioned in the text at appropriate places
 - Standard abbreviations for technical terms and journals should be used
 - All constants should be expressed in **SI units**
 - References should be numbered consecutively and should appear in the text as superscript at appropriate places.
 - References should be in following pattern
 - For research paper:**
Authors' initials and surname, Journal abbreviation, Volume, Page, Year.
 - For book:**
Authors' initials and surname, Book name, Publisher, Place, Year.
 - For proceedings:**
Authors' initials and surname Proceedings' of the conference name, place, Page, Month and Year.
- The paper is to be submitted in word file and PDF file to isasjournal@isasbharat.in
- After getting the acceptance of the paper, authors have to submit **signed copyright form and undertaking** before publishing the article



Indian Society of Analytical Scientists



Message from President ISAS

My heart swells with pride to note that Journal of ISAS (J. ISAS) is going to complete two years of its quarterly e - publication on July 30, 2024.

Pivotal objective of Indian Society of Analytical Scientists (ISAS) was dissemination of science and new researches in the field right from its inception since four decades back in 1983 from the grassroots level, publication being one of the major component of the integrated approach.

The efforts made of bringing out a journal of ISAS during the time (with several limitations) restricted the publication to be sporadic in nature, constrained mostly to the extent of newsletters with a fewer research articles. The constraints took their toll to the extent that intent of publication of a scientific journal slowly crept to subconscious but never dead. The dormant idea started re throbbing, on meeting several ignited minds with equal frequency and the idea crystallised on 30th July, 2022 with e- publication of first issue of peer reviewed quarterly journal J. ISAS free of any charge on either side researcher or reader. The journey began with acquisition of ISSN and DoI (worldwide recognition for individual research paper) numbers for the journal. The journal is open access and accepts diverse array of cutting edge peer reviewed research articles in analytical sciences and allied fields employing state of art techniques for quantification and characterisation.

Today at the verge of celebration of two years of the inspiring journey we must congratulate the stellar performance of perseverance, resilience and sheer determination of the entire group responsible specially in particular Editor in Chief Dr Nilima Rajurkar. The continuing journey is endless. I sincerely wish the journal an endless, successful journey of bringing out newer of researches of immense utility to mankind marking deep impression on scientific community.

Dr.Raghaw Saran
President ISAS and
Advisor J.I SAS



Indian Society of Analytical Scientists.



Editorial

Dear Readers,

We are delighted to present the ninth issue of the Journal of Indian Society of Analytical Scientists (J. ISAS) as we celebrate the second anniversary of our publication. Over the past two years, our journey has been one of growth, innovation, and a steadfast commitment to advancing the field of analytical science. As a peer-reviewed quarterly e-journal with ISSN and DOI numbers, J. ISAS has consistently aimed to provide a platform for high-quality research that drives scientific progress and addresses contemporary challenges.

In this special anniversary issue, we are proud to feature a diverse array of manuscripts that exemplify the breadth and depth of analytical science. It presents a diverse array of innovative research and case studies, each contributing to advancements in forensic science, environmental sustainability, water treatment, pollution control, and the integration of traditional medicine with modern science. The meticulous identification of Delorazepam in suspected Methaqualone contraband highlights the critical role of analytical precision in forensic investigations. The elemental analysis of discarded printed circuit boards reveals efficient methods for silver recovery, emphasizing the environmental and economic benefits of recycling electronic waste. The SWASTIIK technology for water disinfection, combining fennel oil and hydrodynamic cavitation, addresses global clean water challenges with promising results. The exploration of mesoporous biochar from cotton crop residues demonstrates a sustainable approach to environmental remediation by efficiently adsorbing p-nitrophenol. Lastly, a review on the synthesis and characterization of Ayurvedic Bhasmas bridges ancient practices with contemporary science, offering a comprehensive understanding and potential validation of these traditional medicines. Together, these studies underscore the importance of innovative techniques and interdisciplinary approaches in addressing pressing global issues.

This milestone is a testament to the collective efforts of our dedicated editorial board and advisory board, the rigorous contributions of our authors, and the invaluable insights of our reviewers. We extend our heartfelt gratitude to each one of you for your unwavering support and engagement. I would like to extend my sincere gratitude to Dr. Raghav Saran, National President of ISAS and Advisor to J. ISAS, for his invaluable suggestions and support. My Special thanks to the Editors: Dr. Vijayalaxmi Adya and Dr. Vinay Bhandari for their cooperation. The technical assistance provided by Shivani Katak and Vaibhav Parse is greatly appreciated.

The continued support and active participation of our readers, authors, and reviewers are crucial in sustaining the high standards of J.ISAS. We look forward to many more years of fostering scientific excellence and contributing to the global body of knowledge in analytical science. Thank you for being a part of our journey.

Sincerely,



Dr. Nilima Rajurkar
Editor in Chief
J.ISAS

Journal of ISAS

ISSN : 2583-5459 3(1), Pages 1 to 82, (2024)

(An open access Peer reviewed quarterly e- journal by Indian Society of Analytical Scientists)

Contents

S.No.	Title and Authors	Page no.
1	Research Paper: High Surface Area Mesoporous Cotton Crop Biochar for Enhanced Confiscation of <i>p</i>-nitrophenol Priyanka Doondani, Ajay Burile, Aman Bishnani and Ravin Jugade* *Email: ravinj2001@yahoo.co.in DOI: 10.59143/isas.jisas.3.1.QKCW8896	1-20
2	Case Study: Identification of Delorazepam in Suspected Methaqualone Contraband:A Case Study S. P. Deore, S. O. Chetti* and S. V. Ghumatkar *Email - sandeepchetti@gmail.com DOI: 10.59143/isas.jisas.3.1.LBRB1647	21-29
3	Review: From Ancient Practices to Modern Science: A Review on the Synthesis and Characterization of Ayurvedic Bhasmas Nilima Rajurkar*, Shailesh Kantak, Babita Kale *Email: rnilima@rediffmail.com DOI: 10.59143/isas.jisas.3.1.KNFU6221	30-51
4	Short communication: Elemental Analysis of Discarded Printed Circuit Boards using Different Analytical Techniques and Recovery of Silver Yuvaraj Kulkarni *Email: yuvakulkarni985@gmail.com DOI: 10.59143/isas.jisas.3.1.DKBG9369	52-61
5	Research Paper: SWASTIIK Technology for Drinking Water Treatment- Enhancing Water Disinfection Efficacy using Fennel Oil and Hydrodynamic Cavitation Sanyogita N. Berde ^{1,2} , Divya Dixit ¹ , Shilpa S. Chapadgaonkar ² , Vinay M. Bhandari ^{1*} *E-mail: vm.bhandari@ncl.res.in DOI: 10.59143/isas.jisas.3.1.KHHI2753	62-82

High Surface Area Mesoporous Cotton Crop Biochar for Enhanced Confiscation of *p*-nitrophenol

Priyanka Doondani¹, Ajay Burile², Aman Bishnani¹, Ravin Jugade^{1*}

¹Department of Chemistry, RTM Nagpur University, Nagpur-440033, India

²Priyadarshini Bhagwati College of Engineering, Nagpur-440024, India

*Email: ravinj2001@yahoo.co.in

Received: 21.6.2024, Revised: 15.7.2024, Accepted: 20.7.2024

Abstract

This research study investigates the efficacy of utilizing biochar obtained from cotton crop residues for the enhanced remediation of *p*-nitrophenol (PNP). Cotton crop residue-derived biochar (CCB) was prepared using 1N phosphoric acid and subsequently characterized. Batch adsorption experimental analysis were conducted to assess the optimal adsorption capacity of CCB for PNP under various conditions, including temperature, pH, interaction time, initial PNP concentration, and dosage of biochar. The results demonstrated optimal adsorption capacity of 55.38 mg/g at pH 5.0, initial PNP concentration of 100 mg L⁻¹, and biochar dosage of 200 mg at a room temperature of 298 K. The experimental adsorption data exhibited an excellent correlation with the Redlich-Peterson isotherm model. Analysis of the sorption kinetics revealed that the material's uptake behavior closely followed a pseudo-second-order model. Thermodynamics analysis unveiled that the adsorption of PNP onto CCB was exothermic, spontaneous, and primarily driven by enthalpy. Overall, the findings suggest that CCB exhibits promising potential as an efficient adsorbent for the remediation of aquatic environments afflicted with presence of PNP.

Keywords: biochar; adsorption; *p*-nitrophenol; water treatment; organic pollutants.

1. Introduction

Water contamination has become a significant environmental concern, primarily due to the rapid expansion of industrial activities. Effluents discharged from industries such as petrochemicals, pesticides, and coking contain elevated levels of phenol, posing considerable challenges for treatment. The particular concern is the improper disposal of *p*-nitrophenol (PNP) by industries, given its role as an intermediate in the production of insecticides, pharmaceuticals, and other chemical compounds. Significantly, the presence of PNP with substituted hydroxyl (-OH) and nitro (-NO₂) groups is categorized as a highly hazardous contaminant, exerting adverse effects on the surrounding environment¹⁻³. The adsorption method has attracted significant focus in contrast to alternative techniques for eliminating PNP, including membrane separation⁴, extraction⁵, biological methods⁶ and advanced oxidation⁷. This preference is attributed to its perceived safety, operational simplicity, and capacity for reuse without causing secondary pollution⁸. Several adsorbents like activated Kaolinitic clay⁹, HDTMA modified Natural Zeolite¹⁰, ZrSiO₄-MnO₂ nanoparticles¹¹ and Montmorillonite¹² have been reported for the adsorption of PNP, but they often suffer from drawbacks such as low adsorption capacity, high cost, and complicated synthesis processes. Consequently, there is a pressing need to develop adsorbents that are both cost-effective and simple to synthesize for the efficient removal of PNP. In light of this, our research aims to address these issues by focusing on the development of such adsorbent for PNP removal. In recent years, we have reported various adsorbents for eliminating organic pollutants from water¹³⁻¹⁷; however, porous carbon material stands out as one of the most commonly utilized options. Its popularity stems from its extensive accessible surface area, well-established pore network, exceptional physical and chemical resilience, and diverse range of feedstock material sources¹⁸. Currently, porous carbon adsorbents are produced through several methods, encompassing thermal activation, chemical activation, and templating techniques. The thermal activation route involves gaseous substances like CO₂ or moisture in air as activation agents, followed by subsequent processing steps. However, this activation method necessitates elevated temperatures, typically ranging from 800 to 1000 degrees Celsius, resulting in substantial energy consumption^{19,20}. Chemical activation is a valuable method for manufacturing porous carbon materials characterized to elevated specific surfaces and well-developed pore structures. Nevertheless, this process commonly employs corrosive alkaline or acidic activators such as NaOH, KOH, and H₃PO₄.

Biomasses, such as municipal solid waste (MSW), industrial organic waste, and agricultural residue²¹, hold promising potential as natural adsorbents due to their abundant supply and cost-effectiveness^{22,23}. Developing biochar-based sorbents is crucial for environmentally friendly sustainable development and efficient waste water treatment. Biochar, derived from thermal decomposition of biomass feed stocks at elevated temperatures, contains numerous oxygen functional groups (OFGs) and exhibits conductivity in water bodies. Furthermore, extensive research has been conducted on biochar's applications in soil. Combining environmental remediation, carbon sequestration, and affordable sorbents for pathogens and contaminants has garnered significant interest^{10,24}. In the recent years, Zhang et al. utilized rapeseed and cabbage to produce layered double oxides and biochar for phosphate removal from aqueous solutions²⁵. Similarly, Yi et al. developed an adsorbent from rice husk and wood chips using slow pyrolysis to enhance levofloxacin removal²⁶. The results of these studies sparked our interest in synthesizing biochar. The combined research findings highlight biochar's multifaceted capacity as an efficient sorbent material for pollutant extraction.

The Vidarbha region in Central India, well-known for its cotton production, generates significant amounts of cotton straw as a byproduct. Unfortunately, much of this straw is discarded as waste. Recognizing activated carbon's high adsorptive potential due to its extensive surface area, our research was focused on producing biochar from waste cotton stalks. This study focuses on utilizing cotton crop residue-derived biochar (CCB) for the targeted removal of PNP, an organic toxicant.

2. Experimental

2.1. Chemicals

Adsorption experiments were conducted utilizing high-quality reagents and chemicals of analytical grade. *p*-nitrophenol was sourced from LOBA Chemie Pvt. Ltd., while phosphoric acid was procured from SRL, India. Deionized water was utilized for all experimental procedures. It's noteworthy that all the chemicals employed were of high purity, eliminating the need for additional refinement processes.

2.2. Synthesis of cotton crop residue derived biochar

The cotton crop residues underwent thorough cleaning to eliminate absorbed pollutants before being dried under sunlight and in a hot air oven to produce biochar. The synthesis of biochar was conducted following the procedure outlined in the literature with slight adjustments²⁷.

Subsequently, the dried residues were immersed in 1 N phosphoric acid for 24 hours. After treatment with phosphoric acid, the stalks underwent prolonged desiccation process in an hot air oven for extended period of 24 hours. It has now been proved that phosphoric acid treatment prior to pyrolysis leads to enhancement in surface area of biochar. This has been well-established fact that the change in surface area is attributed to crosslinking properties of phosphate ions²⁷. Subsequently the dried material was subjected to pyrolysis in an electric muffle furnace. The pyrolysis was carried out at a high temperature of 600 °C for a time period of five hours, with continuous flow of nitrogen gas at a rate of 150 cubic centimeters per minute. After pyrolysis, biochar derived from cotton crop residues was obtained. This biochar was then mechanically ground to reduce its particle size to approximately 100 microns. The ground biochar was subjected to repeated rinsing with deionized water until the runoff exhibited neutral pH. This material was stored and labeled as cotton crop residue-derived CCB (CCB). Fig.1 illustrates the complete synthesis sequence for CCB.

2.3. Characterization methods

The synthesized CCB underwent comprehensive characterization using various analytical techniques. The surface morphology and structural features of CCB were examined through scanning electron microscopy (SEM), using TESCAN VEGA 3 SBH instrument. To investigate the crystalline nature, X-ray Diffraction (XRD) analysis was conducted using diffractometer system XPERT PRO Miniflex-300/600. This system operated at 300 W power with copper K α radiation, scanning 2 θ range from 1 to 100°. Chemical bond characteristics were investigated using Fourier-Transform Infrared (FT-IR) spectroscopy. A Bruker Alpha-E instrument, featuring a ZnSe attenuated total reflectance ATR crystal, analyzed samples across frequencies from 500 to 4000 cm⁻¹. The specific surface area (SSA) and porosity were evaluated by nitrogen adsorption-desorption measurements on a Quantachrome Nova 2200e BET surface area analyzer. The thermal stability of the synthesized CCB was assessed using a Shimadzu DTG-60 Differential Thermal Analyzer (DTA-TG) under a nitrogen atmosphere, with thermograms noted up to 600°C. Optical measurements were made using UV-Visible spectroscopy, employing a Shimadzu UV-1900i double-beam spectrophotometer functioning across 200 to 900 nm. Solution pH measurements were conducted by means of Equiptronics EQ-615 pH meter.

2.4. Batch Adsorption

Batch adsorption trials were performed to assess the adsorption capability of the newly synthesized CCB. In these experiments, predetermined amount of CCB was introduced into 25 mL of PNP solution with a specific pH and concentration. The mixture was stirred with a magnetic stirrer for a set duration to allow equilibrium to be reached. Following the adsorption period, the mixture was made to undergo separation using Whatman grade 1 filter paper. The residual PNP in the filtrate was quantified using spectrophotometer at 317 nm. The quantity of PNP adsorbed onto the adsorbent (mg/g) was then estimated with the help of mathematical equation (1) presented below:

$$q_e = \frac{C_0 - C_e}{W} \times V \quad (1)$$

The percentage of PNP removal was evaluated using the formula,

$$\% \text{ Removal} = \frac{C_0 - C_e}{C_0} \times 100 \quad (2)$$

Where C_0 represents the initial PNP concentration (mg L^{-1}), C_e stands for equilibrium PNP concentration (mg L^{-1}), W represents CCB weight in g, and V signifies PNP solution volume (L). To validate the reliability of the experimental data, batch adsorption trials were conducted three times independently. The final reported values in the study represent the mean value calculated from the results of these three replicate experiments.

3. Results and discussion

3.1. Characterization

FT-IR spectroscopy can be utilized as an analytical technique to examine the nature of the interactions occurring between the adsorbent material and the p-nitrophenol (PNP) molecules during the adsorption process. The FTIR spectrum exhibited distinct absorption peaks at wave numbers 1577.02 cm^{-1} and 1698.73 cm^{-1} , which can be assigned to the stretching vibrational modes of aromatic C=C and C=O respectively. Additionally, the peaks detected at 1415.68 cm^{-1} , 1197.21 cm^{-1} , and 1160.28 cm^{-1} are indicative of the presence of C-O bonds characteristic of carboxylic acid moieties. The synthesized CCB showed aromatic groups and functional groups rich in oxygen which provide binding sites for the organic pollutant, PNP. Fig.2 represents the FT-IR spectra of the synthesized CCB.

SEM reveals the surface morphology of the CCB. Fig.3 represents SEM images at three different magnifications. SEM analysis of CCB revealed a textured surface morphology

characterized by numerous pores and folded regions. This unique feature, with its high degree of porosity and increased surface roughness, results in an augmented overall surface area for CCB. Consequently, the expanded surface area served to enhance the adsorption capacity of the CCB, enabling more efficient removal of target adsorbate species.

The assessment of surface area relies on the concept of single-layer adsorption-desorption of nitrogen molecules on the material's surface. Concurrently, the BJH technique employs the relationship between pore saturation pressures and nitrogen condensation within cavities to elucidate the pore size distribution of CCB. The CCB porosity characteristics and SSA were investigated through nitrogen sorption experiments, with the resulting equilibrium data as illustrated in²⁸ Fig.4a and 4b. Analysis indicated that the material possessed a considerable surface area of 405.7 m²/g and a noteworthy pore volume of 2.4 × 10⁻¹ cc/g. This remarkable increase in surface area can be linked to the presence of numerous microscopic voids within the material's structure. The mean pore width was calculated as 2.388 nm, indicative of its mesoporous nature. The equilibrium curve aligns with Type IV(a) in the IUPAC categorization system²⁹. The BET equation parameter was determined to be 52.388, suggesting robust interactions between the adsorbate and the material's surface³⁰. The synergy of substantial pore volume and expansive surface area significantly enhances the CCB exceptional capacity for toxicant capture¹⁹.

Thermal stability of synthesized CCB was assessed using TGA-DTA analysis, which provides insights into the material's performance under various thermal conditions. The TGA analysis was conducted by ramping temperature at a controlled rate of 20 °C per minute while maintaining inert nitrogen environment with a continuous flow rate of 100 mL min⁻¹. The TGA curve for CCB revealed a total weight loss of 30% (Fig.4c), indicating good thermal stability. The DTA curve (Fig.4d) showed an endothermic peak corresponding to a weight loss of approximately 2% at 100 °C. This observed reduction in weight results from the release of physically bound water molecule and atmospheric moisture from the CCB around 100 °C. Additionally, the XRD analysis of CCB revealed the presence of well-defined peaks at 2θ = 25.12° and 46.02°, which are characteristic of biochar (Fig.4d). The peaks may be due to cellulose present in cotton crop. The XRD pattern shows that CCB is amorphous in nature.

3.2. Analysis of PNP adsorption studies on CCB

3.2.1. pH zero-point charge (pH_{zpc})

The adsorption behavior of molecule on a surface can be influenced based on the pH relative to the zero-point charge (pH_{zpc}). When the solution pH is below the pH_{zpc} value, the adsorbent acquires a positive surface charge, whereas above the pH_{zpc} , its surface becomes negatively charged³¹. Adsorption occurs for species with a charge opposite to that of the adsorbent surface. To experimentally determine the pH_{zpc} of CCB, a batch equilibration technique was conducted. This involved preparing nine separate mixtures, each containing 25 mL of 0.1 M NaCl solution with initial pH adjusted from 2.0 to 10.0, adjusted using HCl and NaOH. To each mixture, 100 mg of CCB was introduced, and the suspensions were continuously agitated for 24 hours using magnetic stirrers. Subsequently, the final pH of the filtrates was measured for each mixture. By plotting the change in ΔpH ($pH_{initial} - pH_{final}$) against the corresponding initial pH values, the pH_{zpc} for the CCB was revealed to be pH 7.8 (Fig.5a).

3.2.2. Effect of solution pH on PNP adsorption

The pH significantly influences the adsorption of PNP. To investigate this effect, a series of experiments were conducted. Seven beakers were prepared, each containing 25 mL of a 100 mg L⁻¹ PNP solution with pH values spanning from 3.0 to 9.0, adjusted using appropriate acid or base solutions. To each beaker, 100 mg of the CCB was introduced, and the mixtures were continuously agitated for time period of 60 minutes to allow the adsorption process to occur. Following the agitation phase, the mixtures was subjected to separation, and the residual PNP in the filtrate was quantified. The findings indicated that PNP sorption by CCB reached its peak at pH 5.0, as depicted in Fig.5b. As the solution becomes more alkaline, the CCB's surface accumulates negative charges, resulting in electrostatic repulsion between the negatively charged PNP entities and the CCB surface. This interaction diminishes the CCB's-PNP capturing capacity.

3.2.3. Effect of CCB dosage on PNP adsorption

The effect of CCB dosage on PNP sorption was examined by varying the CCB amount from 10 to 400 mg in a 100 mg L⁻¹ PNP solution maintained at pH 5.0. As illustrated in Fig.5c, the PNP-capturing efficiency enhanced with increasing CCB quantity, showing maxima at 200 mg. Subsequent additions yielded no further improvement. This saturation point is explained by the exhaustion of available PNP molecules at the given concentration. The findings indicate

that equilibrium was reached using 200 mg of the CCB, with additional amounts providing negligible benefits to the sorption process. Based on these observations, 200 mg was identified as the ideal quantity for subsequent sorption experiments.

3.2.4. Effect of interaction time

The influence of interaction time was assessed by altering the exposure time from 10 to 180 minutes for a 100 mg L⁻¹ PNP solution (pH 5.0) with 100 mg of the CCB. The results are depicted in Fig.5d. Peak sorption occurred with 60 minutes of interaction time, at which point equilibrium was achieved³². Consequently, 60 minutes was determined to be the ideal interaction time for subsequent experiments.

3.2.5. Effect of initial PNP concentration

To determine the sorption capacity of CCB, 25 mL of PNP solutions with varying concentrations from 10 to 300 mg L⁻¹ of pH 5.0 were prepared in individual beakers. Each beaker received 50 mg of CCB, and the mixtures were agitated continuously for 60 minutes. After agitation, the solutions were filtered, and the % removal of PNP was assessed. It was observed that the % removal was approximately 60% for concentrations up till 100 mg L⁻¹, but it decreased as the PNP concentration increased further. This trend is expected because higher PNP concentrations lead to fewer available adsorption sites on the adsorbent³³. Therefore, a 100 mg L⁻¹ concentration of PNP was selected for further investigations (Fig.5e).

3.3. Adsorption isotherms

Isotherm analysis were conducted to investigate sorption behavior of PNP onto CCB surface. These experiments involved varying the initial PNP concentration levels from 10 to 300 mg L⁻¹ at pH 5.0, using 50 mg CCB dose, at 298 K for 60 minutes. The resulting data was analyzed utilizing various isotherm models, as presented in Table 1. The regression coefficient for both Langmuir and Redlich-Peterson (R-P) isotherm models were found to be very close to 1.0, suggesting the potential formation of a PNP monolayer on the homogeneous CCB surface³⁴. (Fig.6a displays the best fitted isotherm model curve). Also, it can be observed from Table 1, that the χ^2 value for R-P isotherm is low, affirming that R-P isotherm is followed. The value of $R_L = 0.034$, being less than one, indicating favorable adsorption conditions. Furthermore, the Freundlich isotherm model parameter $n = 3.462$ suggests chemisorption process³⁵. Additionally, the positive value of Temkin isotherm constant $b = 299.2 \text{ J mol}^{-1}$ signifies that

the adsorption process is exothermic^{36,37}. The Redlich-Peterson model, which incorporates elements from both Langmuir and Freundlich isotherms approaches, provided the most accurate representation of the experimental results, suggesting that the process does not strictly adhere to ideal monolayer behavior³⁸.

The Table 1 compares the adsorption capacities of the synthesized CCB material with other adsorbents reported in literature for the removal of p-nitrophenol (PNP). As evident from the tabulated data, the CCB adsorbent demonstrates a remarkably high adsorption capacity towards PNP, outperforming various other adsorbent materials investigated for this application.

3.4. Adsorption kinetics

Adsorption kinetics provides insight into the rate at which the adsorption process progresses as a function of contact time (Fig. 7). The pseudo-first-order (PFO) kinetic model describes the rate of adsorption using the following rate expression⁴²:

$$\log(q_e - q_t) = \log q_e - \left(\frac{k_1 t}{2.303}\right) \quad (3)$$

Where q_e (mg g⁻¹) is the amount of adsorbate adsorbed at equilibrium, q_t (mg g⁻¹) is the amount adsorbed at time t , the amount of PNP adsorbed at a certain time t and k_1 (min⁻¹) is the PFO rate constant.

The pseudo-second-order (PSO) kinetic model, on the other hand, employs the following rate equation⁴³:

$$\frac{t}{q_t} = \frac{1}{k_2 q_e^2} + \frac{t}{q_e} \quad (4)$$

Where k_2 (g mg⁻¹ min⁻¹) represents the PSO rate constant. Analysis of the correlation coefficients (R^2) revealed that the PSO model provided the best fit to the experimental kinetic data (Table 3). Additionally, the intraparticle diffusion (IPD) model suggested that pore diffusion is the rate-limiting step, as adsorbate ions can potentially diffuse into the adsorbent pores facilitated by magnetic stirring⁴⁴. In the Weber Morris IPD model, the rate-determining step involves permeation of PNP from the bulk liquid phase to the solid surface of CCB. The rate expression for this model is as:

$$q_t = k_{int} \cdot t^{1/2} + C \quad (5)$$

Where k_{int} (mg g⁻¹ min⁻¹) denotes the intraparticle diffusion rate constant, and C is a constant related to the boundary layer effect. The non-zero intercept obtained from the plot (Fig. 7c)

indicates that both the diffusion process and the boundary layer play crucial roles in the rate-determining step⁴⁵. Furthermore, the kinetic profile exhibits two distinct linear regions, suggesting an initial rapid diffusion phase followed by a gradual approach to equilibrium after 60 minutes. This is in agreement with various studies reported in literature⁴⁶.

3.5. Adsorption thermodynamics

The effect of temperature on PNP adsorption was investigated at different temperatures, specifically varying from 301 K to 316 K, using a temperature-controlled magnetic stirrer. Fig.5f indicates that temperature has a minor effect on the percentage removal. By examining the impact of temperature, it is possible to calculate various thermodynamic parameters. These parameters are essential for understanding the spontaneity and driving forces of the adsorption process.

The change in Gibbs free energy (ΔG) for the PNP adsorption process was calculated from the equilibrium constant K with the help of following equation (6):

$$\Delta G^\circ = -RT \ln K \quad (6)$$

The vant Hoff equation gives a relation between change in enthalpy (ΔH) and change in entropy (ΔS) by equation (7):

$$\ln K = \frac{\Delta S^\circ}{R} - \frac{\Delta H^\circ}{RT} \quad (7)$$

In these equations, R represents universal gas constant, T is the absolute temperature (K), ΔH is enthalpy change (kJ mol^{-1}), ΔG is Gibbs free energy change (kJ mol^{-1}), ΔS is entropy change ($\text{J mol}^{-1} \text{K}^{-1}$) and K is the equilibrium constant derived from the ratio of the amount of PNP adsorbed at equilibrium to the equilibrium PNP concentration in the liquid phase. The van't Hoff plot (Fig. 7d) provides the values for ΔH and ΔS , as listed in Table 4. The negative Gibbs free energy change indicates the spontaneity of the process. Additionally, the negative enthalpy change confirms that the process is exothermic, while the negative entropy change suggests a reduction in disorder during the adsorption activity. Given that the change in enthalpy is significantly more negative compared to $T\Delta S$, it can be concluded that this adsorption process is predominantly driven by enthalpy³¹.

4. Conclusion

The cotton crop residue derived CCB was effectively synthesized by phosphoric acid treatment method. BET surface analysis characterization of the material revealed that the CCB has a mesoporous surface with a high pore volume and a surface area of $405.7 \text{ m}^2/\text{g}$. This

composite serves as an excellent adsorbent, demonstrating an adsorption capacity of 55.38 mg of PNP per gram of CCB. The exceptional adsorption capacity arises from the CCB's high surface area and strong CCB-PNP interactions. Adsorption isotherm studies indicated that Redlich-Peterson isotherm model was followed. The thermodynamic evaluation affirmed the spontaneous nature of the adsorption process, governed predominantly by enthalpic contributions, while kinetic investigations suggested that the rate of adsorption adheres to a pseudo-second-order kinetic model. The produced material is cost-effective, environmentally friendly, and an efficient adsorbent for removing the organic pollutant PNP from industrial waste water. This research presents a novel approach, highlighting the potential application of CCB in water purification efforts.

Acknowledgements

Facilities provided by RTM Nagpur University are gratefully acknowledged. We are thankful to DST and UGC for funding under DST-FIST and UGC-SAP programs.

Figures:

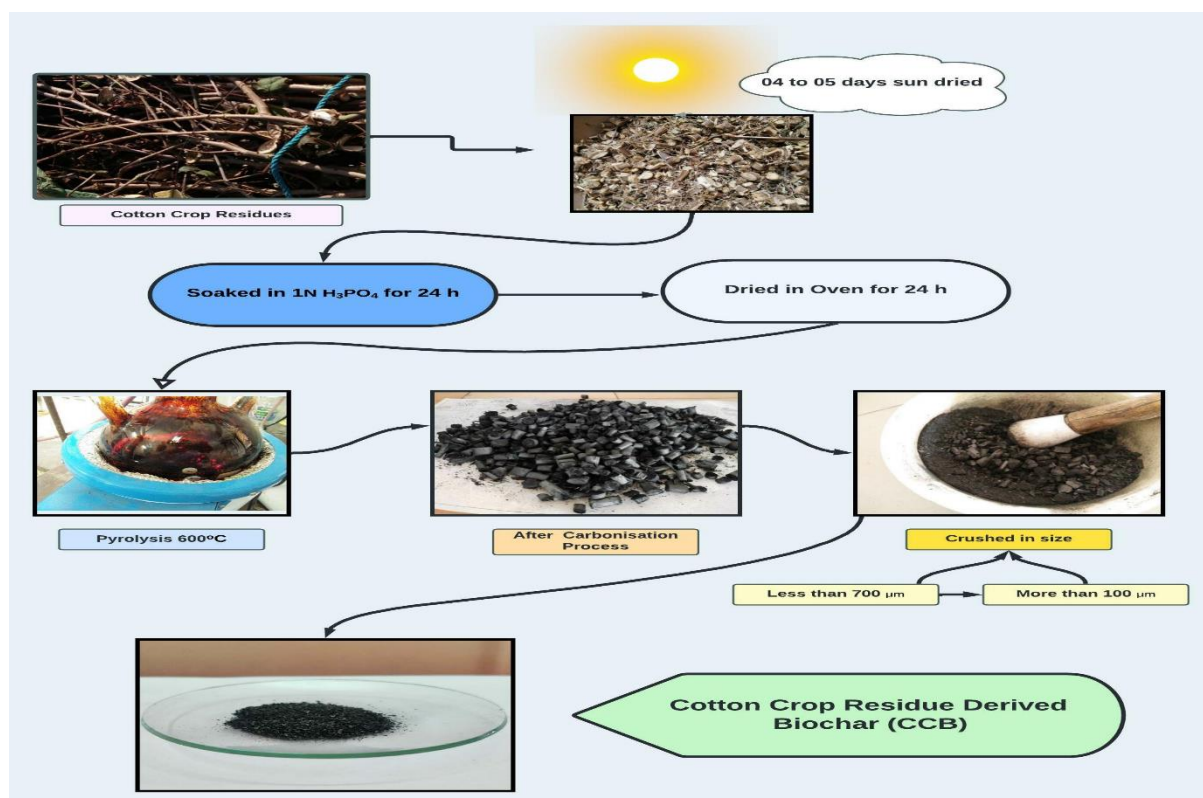


Fig. 1: Process flow diagram for synthesis of Cotton Crop Biochar (CCB)

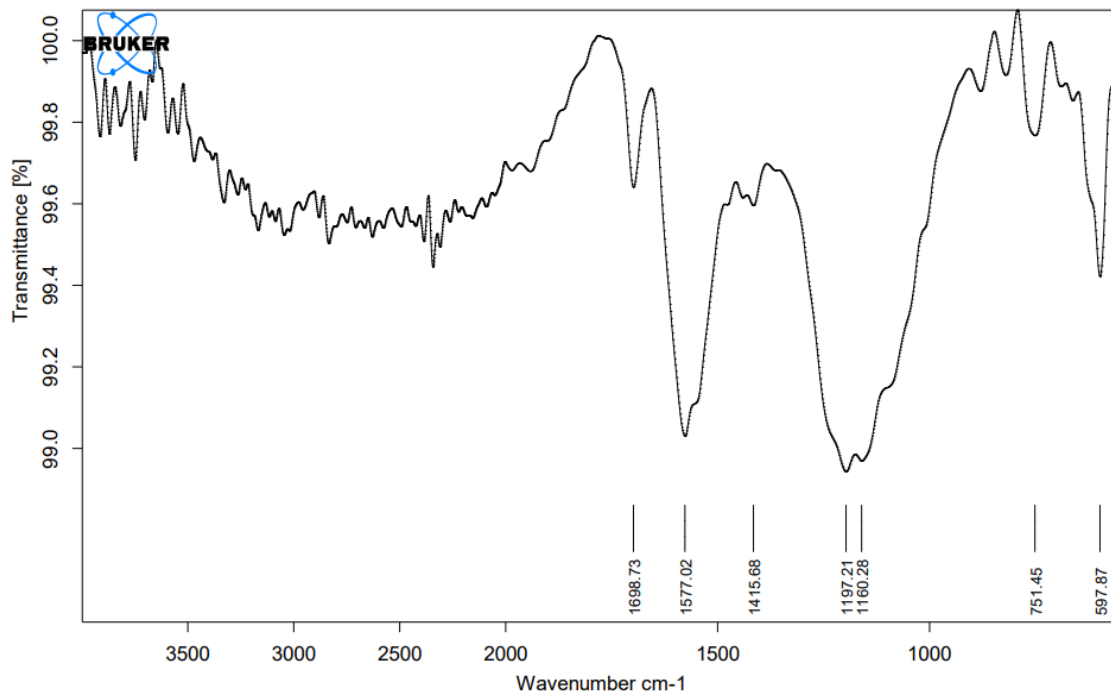


Fig. 2: FT-IR spectrum of CCB

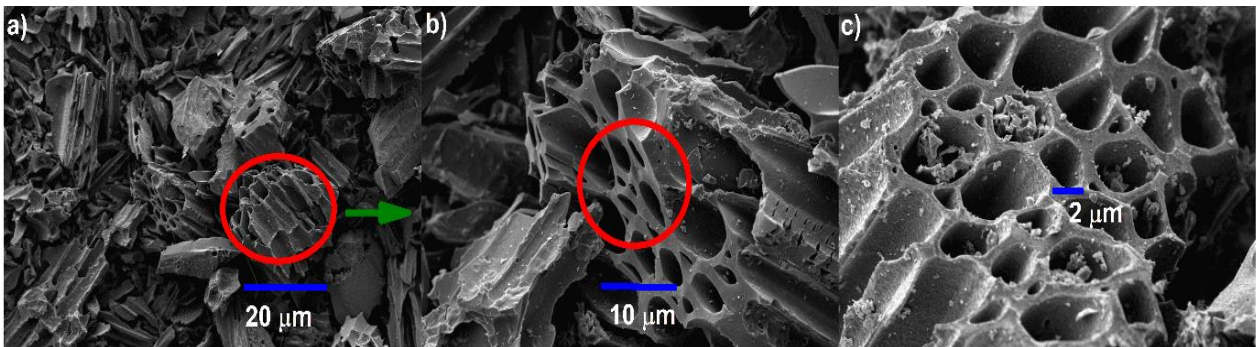


Fig. 3: SEM micrographs of CCB at three varying magnification levels a) 20 μm b) 10 μm c) 2 μm.

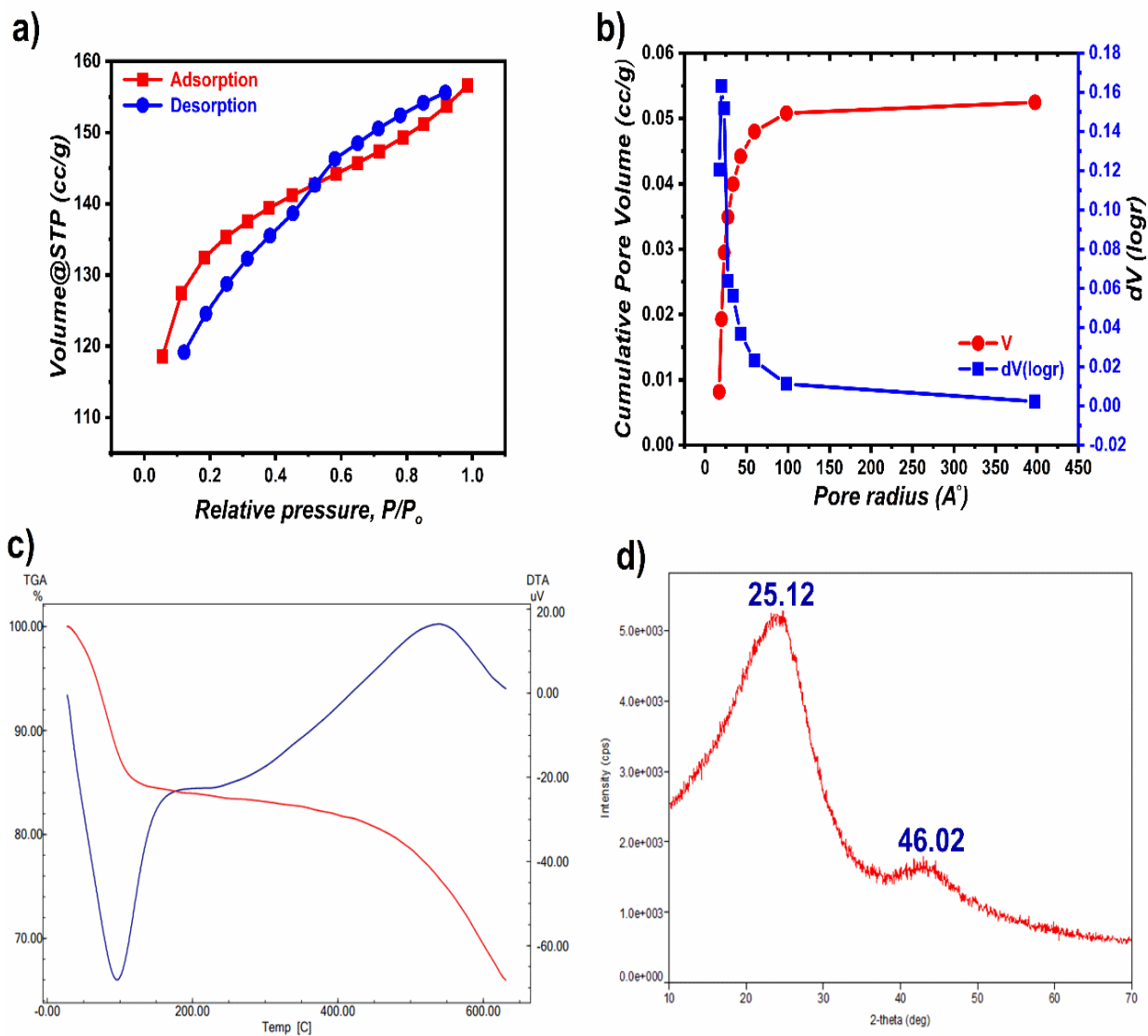


Fig. 4: a) Nitrogen sorption isotherm for CCB b) pore dimension distribution profile of CCB c) TGA-DTA analysis graphs of CCB d) XRD spectrum of CCB

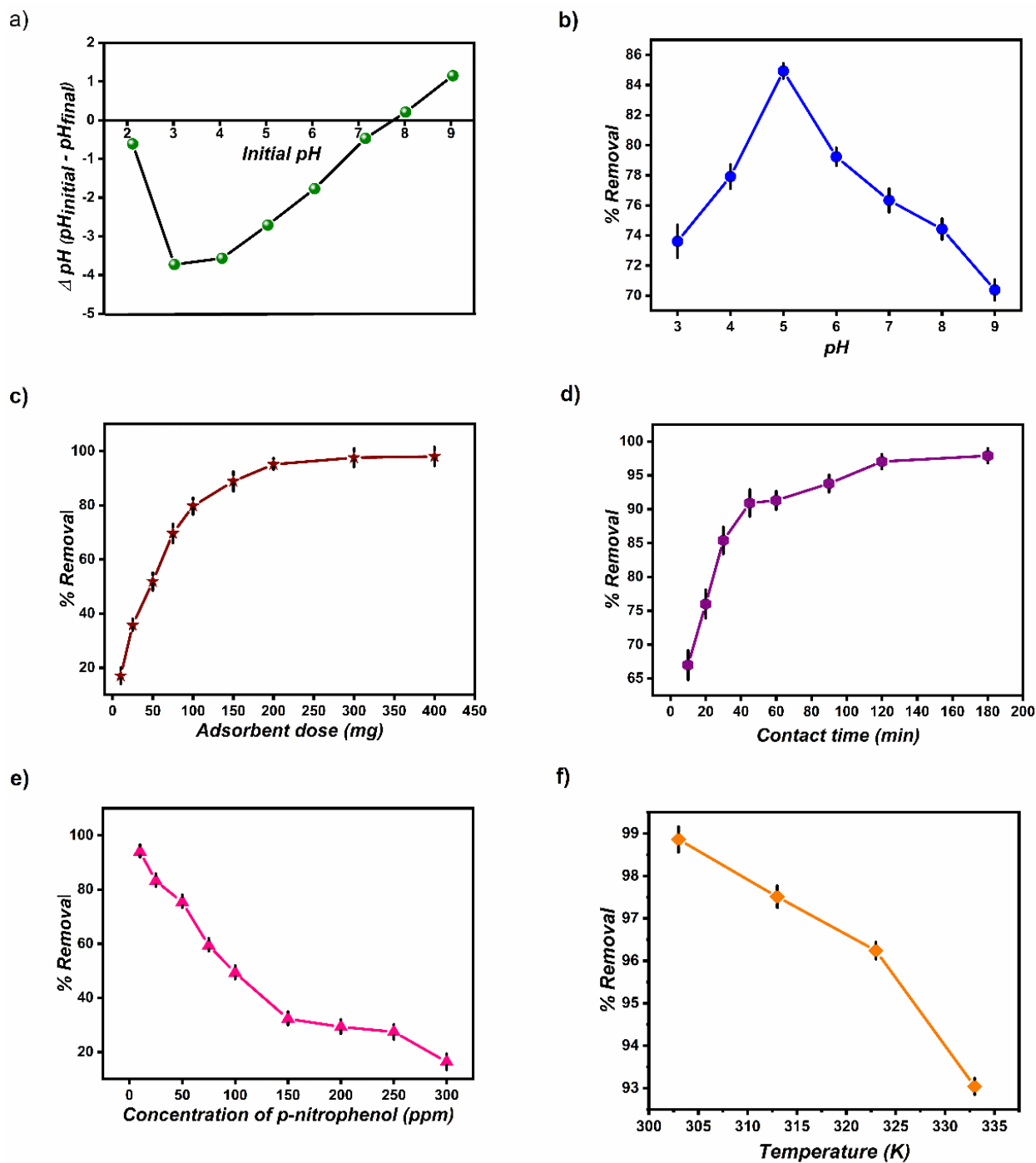


Fig. 5: a) pH_{zpc} curve of CCB b) effect of solution pH on PNP adsorption c) effect of CCB dosage on PNP adsorption d) effect of interaction time and e) effect of initial PNP concentration f) effect of temperature

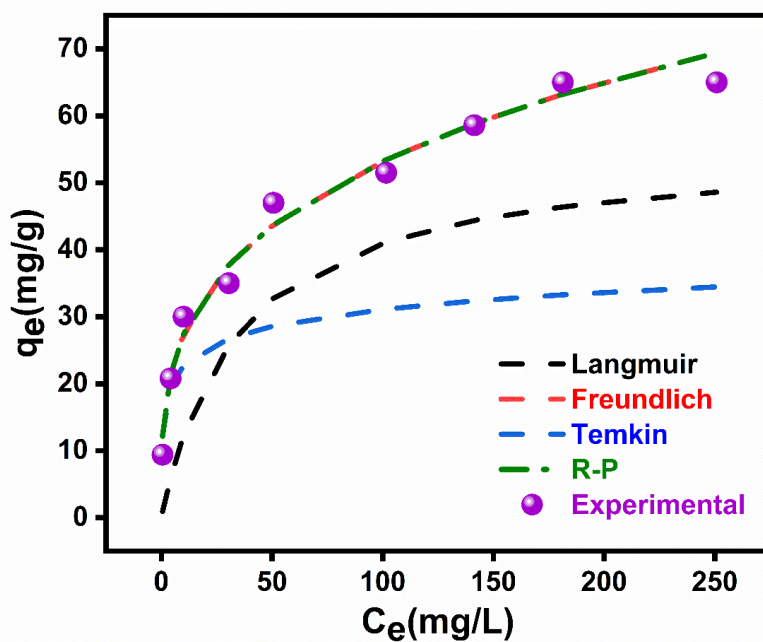


Fig. 6: C_e - q_e curves for comparative analysis of different isotherm models and experimental values for PNP adsorption onto CCB.

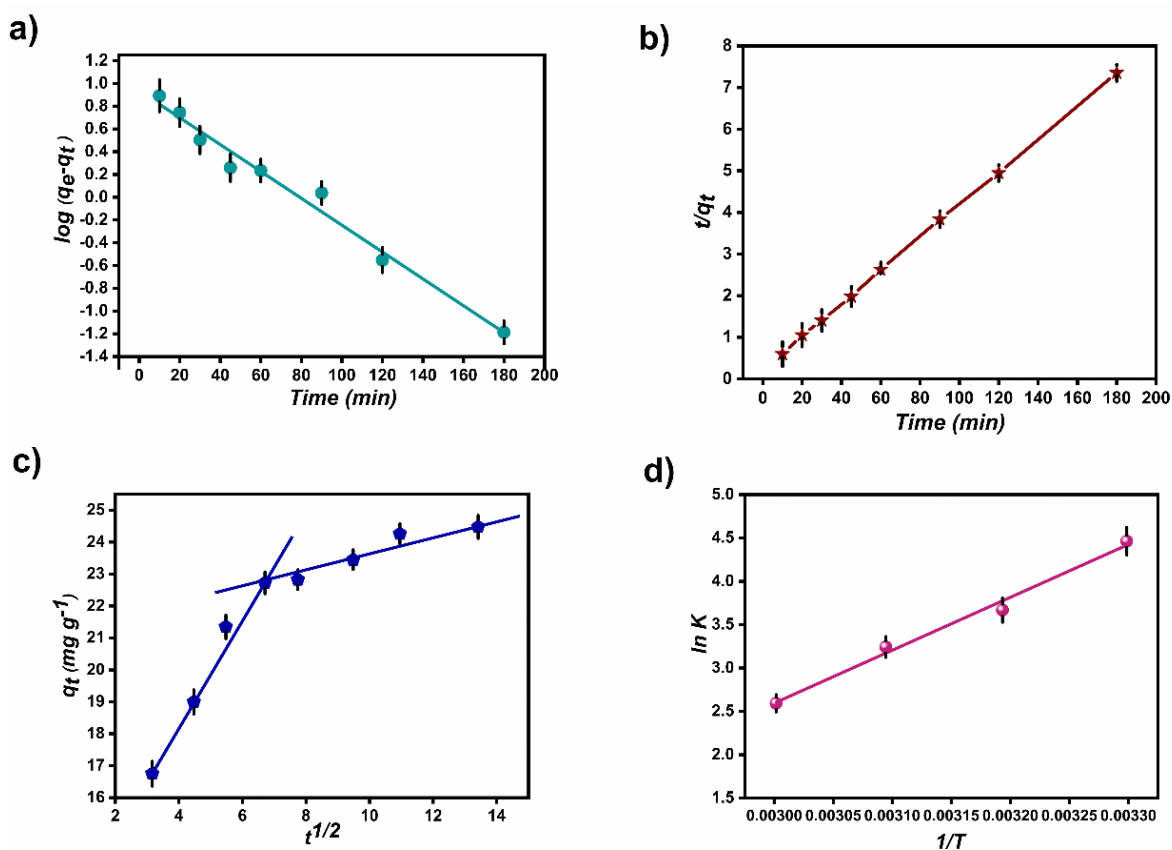


Fig. 7: (a) PFO plot, (b) PSO plot, and (c) IPD model plot (d) van't Hoff plot

Tables:

Table 1: Isotherm modeling parameters for adsorption of PNP onto CCB.

Model	Mathematical Parameters	Obtained values
Langmuir	q_m (mg g ⁻¹)	55.38
	b (L g ⁻¹)	0.282
	R_L	0.034
	R^2	0.961
	χ^2	1810.1
Freundlich	K_F (mg ^{1-1/n} g ⁻¹ L ⁻¹)	14.07
	N	3.462
	R^2	0.875
	χ^2	59.32
Temkin	b (J mol ⁻¹)	299.2
	A_T (L g ⁻¹)	5.436
	R^2	0.867
	χ^2	3510.5
Redlich-Peterson	b	0.711
	A	14.07
	R^2	0.977
	χ^2	59.32

Table 2: Comparison of highest PNP sorption capacities (q_m) onto various adsorbents at different pH values, along with the best-fit isotherm models.

Adsorbent	pH	Isotherm followed	q_m (mg/g)	References
Activated Kaolinitic clay	8.0	Freundlich	0.281	9
HDTMA modified Natural Zeolite	10.0	Langmuir	2.53	10
ZrSiO ₄ -MnO ₂ nanoparticles	4.0	Langmuir	12.09	11
Montmorillonite	3.0	Langmuir	15.30	12
Graphene	6.0	Langmuir	15.5	39
PDNH Nanocomposite hydrogel	7.0	Langmuir	19.20	40
CD@Si Composite materials	8.5	Freundlich	41.5	41
CCB	5.0	R-P	55.38	This study

Table 3: Kinetic parameters for PNP adsorption by CCB.

Kinetics model	Mathematical constants	Values obtained
PFO	k_1 (min^{-1})	0.0272
	R^2	0.9800
PSO	k_2 ($\text{g mg}^{-1} \text{min}^{-1}$)	0.0073
	R^2	0.9990
IPD	k_i ($\text{mg g}^{-1} \text{min}^{-0.5}$)	0.6995
	C	16.4800
	R^2	0.7940

Table 4: Thermodynamic parameters

T(K)	ΔG (kJ mol^{-1})	ΔH (kJ mol^{-1})	ΔS ($\text{J mol}^{-1} \text{K}^{-1}$)
303	-11.13	-50.72	-130.5
313	-9.825		
323	-8.519		
333	-7.213		

References

1. L. M. Cotoruelo, M. D. Marqués, F. J. Díaz, J. R. Mirasol, J. J. Rodríguez, and T. Cordero, *Chem. Eng. J.*, 184, 176, 2012.
2. G. Xue, M. Gao, Z. Gu, Z. Luo, and Z. Hu, *Chem. Eng. J.*, 218, 223, 2013.
3. Y. Zhou, X. Liu, L. Tang, F. Zhang, G. Zeng, X. Peng, L. Luo, Y. Deng, Y. Pang, and J. Zhang, *J. Hazard Mater.*, 333, 80, 2017.
4. W. Raza, J. Lee, N. Raza, Y. Luo, K.H. Kim, and J. Yang, *J. Ind. Eng. Chem.*, 71, 1, 2019.
5. B. Cui, J. C. Gong, M. H. Duan, Z. X. Chang, L. L. Su, W. J. Liu, and D. L. Li, *J. Chem. Eng. Data.*, 61(2), 813, 2016.
6. X. Zhang, Y. S. Yang, Y. Lu, Y. J. Wen, P. P. Li, and G. Zhang, *Water Res.*, 144, 616, 2018.
7. X. Dong, Z. Gan, X. Lu, W. Jin, Y. Yu, and M. Zhang, *Chem. Eng. J.*, 277, 30, 2015.
8. G. Wang, H. Xiao, J. Zhu, H. Zhao, K. Liu, S. Ma, S. Zhang, and S. Komarneni, *Environ. Res.* 201, 111496, 2021.
9. S. O. Azeez, and F. Adekola, *Pak. J. Anal. Environ. Chem.*, 17, 93, 2016.
10. J. Y. Guo, and B. Wang, *Huanjing Kexue Environ. Sci.*, 37, 1852, 2016.
11. M. E. Mahmoud, and G. M. Nabil, *J. Mol. Liq.*, 240, 280, 2017.
12. M. Houari, B. Hamdi, O. Bouras, J. C. Bollinger, and M. Baudu, *Chem. Eng. J.*, 255, 506, 2014.
13. P. Nandanwar, R. Jugade, V. Gomase, A. Shekhawat, A. Bambal, D. Saravanan, and S. Pandey, *J. Compos. Sci.*, 7, 103, 2023.
14. P. Doondani, R. Jugade, V. Gomase, A. Shekhawat, A. Bambal, and S. Pandey, *Water*, 14, 3411, 2022.
15. P. Doondani, V. Gomase, D. Saravanan, and R. Jugade, *Results Eng.*, 247, 100515, 2022.
16. P. Doondani, D. Panda, V. Gomase, K. R. Peta, and R. Jugade, *Environ. Res.*, 247, 118228, 2024.
17. P. Nandanwar, D. Saravanan, P. Bakshe, and R. Jugade, *Mater. Adv.*, 3, 5488, 2022.
18. G. Singh, J. M. Lee, G. Kothandam, T. Palanisami, A. A. H. Al-Muhtaseb, A. Karakoti, J. Yi, N. Bolan, and A. Vinu, *Bull. Chem. Soc. Jpn.*, 94(4), 1232, 2021.
19. S. Ahmed, J. Pan, M. Ashiq, D. Li, P. Tang, and Y. Feng, *Inorg. Chem. Front.*, 6, 1952, 2019.

20. C.I. Contescu, S.P. Adhikari, N.C. Gallego, N.D. Evans, and B.E. Biss, *J. Carbon Res.*, 4, 51, 2018.
21. W. Ding, X. Dong, I. M. Ime, B. Gao, and L. Q. Ma, *Chemosphere*, 105, 68, 2014.
22. M. B. Ahmed, J. L. Zhou, H. H. Ngo, and W. Guo, *Sci. Total Environ.*, 532, 112, 2015.
23. D. Mohan, A. Sarswat, Y. S. Ok, and C. U. Pittman Jr., *Bioresour. Technol.*, 160, 191, 2014.
24. T. Sizmur, T. Fresno, G. Akgul, H. Frost, and E. Moreno-Jimenez, *Bioresour. Technol.*, 246, 34, 2017.
25. Z. Zhang, L. Yan, H. Yu, T. Yan, and X. Li, *Bioresour. Technol.*, 284, 65, 2019.
26. S. Yi, B. Gao, Y. Sun, J. Wu, X. Shi, and B. X. Hu, *Chemosphere*, 150, 694, 2016.
27. G. Chu, J. Zhao, Y. Huang, and D. Zhou, *Env. Pollut.* 240, 1, 2018.
28. S. Brunauer, P. H. Emmett, and E. Teller, *J. Am. Chem. Soc.*, 60, 309, 1938.
29. M. Thommes, K. Kaneko, A. Neimark, J. Olivier, F. Rodriguez-Reinoso, J. Rouquerol, and K. Sing, *Pure Appl. Chem.*, 87, 1051, 2015.
30. M. Thommes, B. Smarsly, M. Groenewolt, P. I. Ravikovitch, and A. V. Neimark, *Langmuir*, 22, 756, 2006.
31. S. Korde, S. Tandekar, and R. Jugade, *J. Env. Chem. Eng.*, 8, 104360, 2020.
32. S. Kahu, D. Saravanan, and R. Jugade, *Water Sci. Technol.*, 70, 2047, 2014.
33. S. H. Vithalkar, and R. M. Jugade, *Mater. Today: Proc.*, 29, 1025, 2020.
34. I. Langmuir, *J. Am. Chem. Soc.*, 40, 1361, 1918.
35. H. Freundlich, *Z. Phys. Chem.*, 57, 385, 1906.
36. O. Ferrandon, H. Bouabane, and M. Mazet, *J. Water Sci.*, 8, 183, 1995.
37. G. Nechifor, D. Pascu, M. Neagu, G. A. Traistaru, P. C. Albu, *U.P.B. Sci. Bull., Series B.* 77, 1454, 2015.
38. N. Ayawei, A. N. Ebelegi, and D. Wankasi, *J. Chem.*, 3039817, 2017.
39. A. I. Ismail, *Can. J. Chem.*, 93, 1083, 2015.
40. M. T. Nakhjiri, G. B. Marandi, and M. Kurdtabar, *J. Environ. Chem. Eng.*, 9, 105039, 2021.
41. H. M. Shen, G. Y. Zhu, W. B. Yu, H. K. Wu, H. B. Ji, H. X. Shi, Y. B. She, and Y. F. Zheng, *Appl. Surf. Sci.*, 356, 1155, 2015.
42. S. Lagergren, and K. Sven. *Vetensk. Handl.*, 24, 1, 1898.
43. Y. S. Ho, and G. McKay, *Chem. Eng. J.*, 70, 115, 1998.
44. W. Weber, and J. Morris, *J. Sanitary Eng. Div.*, 89, 1, 1963.

45. A. Shekhawat, S. Kahu, D. Saravanan, and R. Jugade, *Int. J. Biol. Macromol.*, 80, 615, 2015.
46. P. M. Nandanwar, S. H. Vithalkar, P. Bakshe, A. Shekhawat, and R. M. Jugade, *J. ISAS*, 1, 35, 2022.

Identification of Delorazepam in Suspected Methaqualone Contraband: A Case Study

S. P. Deore, S. O. Chetti and S. V. Ghumatkar

Directorate of Forensic science Laboratories, Vidyanagari Kalina, Mumbai -400098

*Email - sandeepchetti@gmail.com

Received: 15.6.2024, Revised: 3.7.2024, Accepted: 6.7.2024

Abstract

The present case study reports the analysis of seized narcotic drug received from investigation agency in Mumbai. The drug was suspected to be methaqualone which falls under NDPS act 1985. Analysis of the drug was carried out using HPTLC, GC-MS, UV and Raman spectroscopy techniques. These complimentary techniques revealed and confirmed the presence of delorazepam in the suspected sample while methaqualone was found to be absent. The case study highlights the importance of analytical techniques in identifying the narcotic drug in the seized sample.

Keywords- Delorazepam, Methaqualone, NDPS act 1985, Forensic sample, Commercial Quantity

1.Introduction

Analytical techniques in forensic sciences play a crucial role in the identification and characterization of drugs, which is essential for law enforcement and legal proceedings. These techniques, such as Gas Chromatography-Mass Spectrometry (GC-MS), High-Performance Thin Layer Chromatography (HPTLC), and Fourier Transform Infrared Spectroscopy (FTIR) allow forensic analysts to accurately detect and quantify the presence of controlled substances in various samples. By providing detailed chemical fingerprints of substances, these methods enable the distinction between closely related compounds and the precise determination of drug purity. This level of specificity is critical not only for identifying the type of drug present in a sample but also for tracing its origin and understanding its potential effects, thereby aiding in criminal investigations, and contributing to the establishment of forensic evidence in court

cases. The present paper demonstrates the role of analytical techniques in identifying the suspected drug received from the investigation agency.

Among the various analytical techniques, GC-MS is crucial in forensic science for several reasons. It provides highly accurate and reliable results, which are essential in legal contexts. It can identify and quantify various substances, including drugs, toxins, and explosives, with great precision. This accuracy helps in determining the cause of death, identifying unknown substances, and linking evidence to crime scenes or suspects. GC-MS results are widely accepted in courts due to their robustness and reliability. The technique's credibility and the ability to withstand legal scrutiny make it indispensable in forensic investigations. Maurer et al.¹ have discussed the identification and differentiation of benzodiazepine drugs in urine samples using GC-MS. Maudens et al.² have reported unexpected benzodiazepine findings in three forensic toxicological cases using GC-MS technique. Other case studies, such as the detection of dextropropoxyphene in a suspected opium sample and the detection of alprazolam in a suspected heroin sample, have been documented by our laboratory.^{3,4}

Other analytical techniques such IR, Raman, and UV also play an important role in forensic investigations: Neville et al.⁵ have described the vibrational spectra (IR and Raman) of benzodiazepines, including Raman spectra wavenumbers for some of these compounds. Additionally, Bumrah et al.⁶ provided an overview of the developments in the analysis of drugs of abuse using Raman spectroscopy for forensic purposes and the application of this instrument in characterizing drugs. Atole et al.⁷ detailed a UV spectrophotometric method for drug analysis, including theoretical and mathematical expressions and some applications.

The Forensic Science Laboratory (FSL) receives samples seized under the Narcotic Drugs and Psychotropic Substances (NDPS) Act 1985. These narcotic drugs or psychotropic substances are typically confiscated by investigating officers based on tips. Initial identification of these samples is performed on-site using color tests with available kits. These preliminary tests are not confirmatory; hence, the samples are sent to the FSL for further analysis. The investigation agency in Mumbai seized 485 g drugs suspected as methaqualone which falls under NDPS act 1985. Our laboratory had received 4.83 g of this suspected sample of methaqualone for further examination.

The United Nations Office of Drugs and Crime (UNODC) has recommended various methods for analyzing the narcotic drugs^{8,9}. Systematic analysis of suspected drug using various analytical techniques in our laboratory revealed that suspected sample was not methaqualone

but Delorazepam which also falls under NDPS act 1985. The commercial quantity was decided on the basis of Potency of the drugs i.e. the commercial quantity is less for more potent drug.

2 Experimental

2.1 Chemicals and reagents

AR grade Benzene, acetonitrile, methanol, potassium iodide, bismuth sub nitrate and acetic acid of Sigma Aldrich were used for the analysis of the sample. Dragendorff's reagent was prepared by using potassium iodide, bismuth sub nitrate and acetic acid which was used as spraying reagent for HPTLC plate of silica.

2.2 Procedure

The suspected methaqualone sample received was white powder. Solubility studies on it revealed that it is completely soluble in methanol and insoluble in water. Very small quantity of sample was taken on spot tile and three drops of cobalt thiocyanate reagent was added which showed no colour change indicating absence of methaqualone in sample contraband. In order to further identify and confirm the suspected drug, analysis of the sample was done using various analytical techniques. 1 mg/10mL of sample in methanol was taken for GC-MS and HPTLC analysis.

2.3 High Performance Thin Layer Chromatography

1 mg/ 10mL of standard methaqualone was taken for analysis. Standard and sample were spotted on precoated HPTLC silica plate and the plate was developed in solvent system Benzene: Acetonitrile: Methanol (8:1: 1). Thereafter, Dragendorff's reagent was sprayed on HPTLC plate.

2.4 Ultra -Violet spectrophotometer

UV spectrophotometer of Thermofisher was used. A UV spectrum of sample in methanol showed λ_{max} at 227.9 nm and 319.7nm.

2.5 Gas Chromatography – Mass spectroscopy

GC-MS of Agilent technologies was used for analysis. 1mg/mL of sample in methanol was taken for analysis, 2 microliter sample was injected in GC and following conditions were kept for GC- MS.

Inlet temperature- 150 °C, MS temperature-230 °C, QP temperature-250 °C, Helium was used as carrier gas at 1mL/min flow, HP-5ms capillary column of 30m length. The mass spectra showed presence of delorazepam.

2.6 Raman spectra

Raman spectrometer with microscope of Renishaw technologies was used. The FT- Raman spectra of sample were recorded after the laser beam is focused on the sample operating at 783 nm.

3.0 Results and Discussion

Suspected narcotic drug methaqualone sample was analyzed using different analytical techniques. However, initial screening test showed absence of methaqualone. Further it was confirmed by HPTLC analysis which revealed absence of this drug in suspected sample (Fig. 1). 1mg/mL sample was prepared and spotted on high performance thin layer chromatography (HPTLC). The plate was developed in solvent system benzene: acetonitrile: methanol (8:1:1) and further observed under UV at 250 nm. The observations noted in Table 1 revealed that sample does not contain methaqualone. 2 μ l of above sample was then injected to GC-MS, which showed sharp peak at RT- 23.62 min and the mass spectra of same peak showed mass spectrum primary ions at m/z 304, 275, 269,241,205,186,177,138,120,102,89,75,63 which exactly match with delorazepam as depicted in Figs. 2 and 3.

UV Visible spectra of sample solution in methanol showed λ_{max} at 227.9 nm and 319.7 nm (Fig.4) which are characteristic of delorazepam it tallies with literature value 227 and 319. The sample was further analyzed using Raman spectroscopy. The spectra obtained are shown in Fig. 5. and the Raman shift data are presented in Table 2. An examination of different peaks obtained reveals presence of delorazepam in the suspected sample.

The commercial quantity and small quantity of drugs are mentioned in NDPS act 1985. Depending upon the quantity, the granting bail and/or punishment is decided by Judiciary. Commercial quantity of methaqualone is mentioned as 500 g and that of delorazepam as 100 g. The seized quantity by investigating agency was 485 g, hence the seized quantity can be considered as commercial quantity. The commercial quantity was decided on the basis of Potency of the drugs i.e. the commercial quantity is less for more potent drug. The seized quantity of delorazepam was more potent than that of methaqualone.

Conclusion

The suspected methaqualone drug received from the investigating agency was analyzed in our laboratory using HPTLC, GC-MS, UV, and Raman spectroscopy techniques. The results

revealed the presence of Delorazepam and not methaqualone, in the suspected sample. This work demonstrates the crucial role of analytical techniques in forensic cases.

Figures:

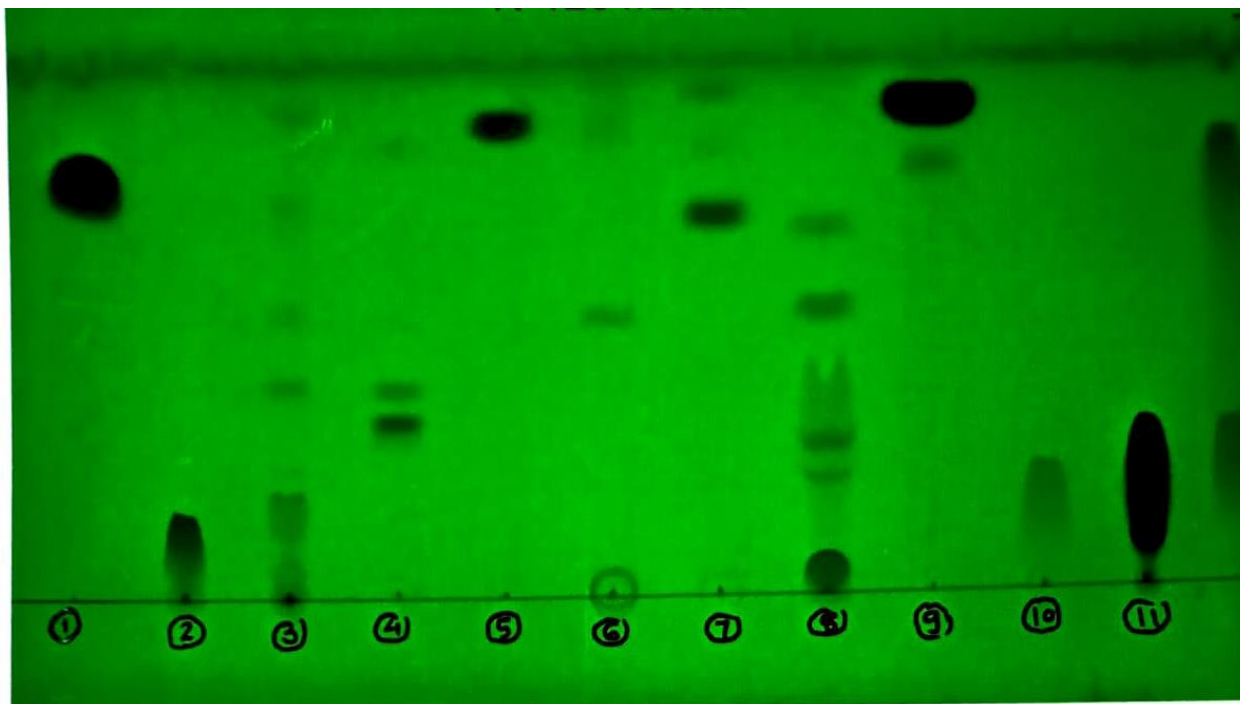


Fig. 1: HPTLC plate of contraband sample

1- Contraband sample, 2-Control Morphine, 3-Control Opium, 4-Control Alprazolam, 5-Control Diazepam, 6-Control Lorazepam, 7-Control Nitrazepam, 8-Control Cocaine, 9-Control Methaqualone, 10-Control Methamphetamine, 11-Control Ketamine

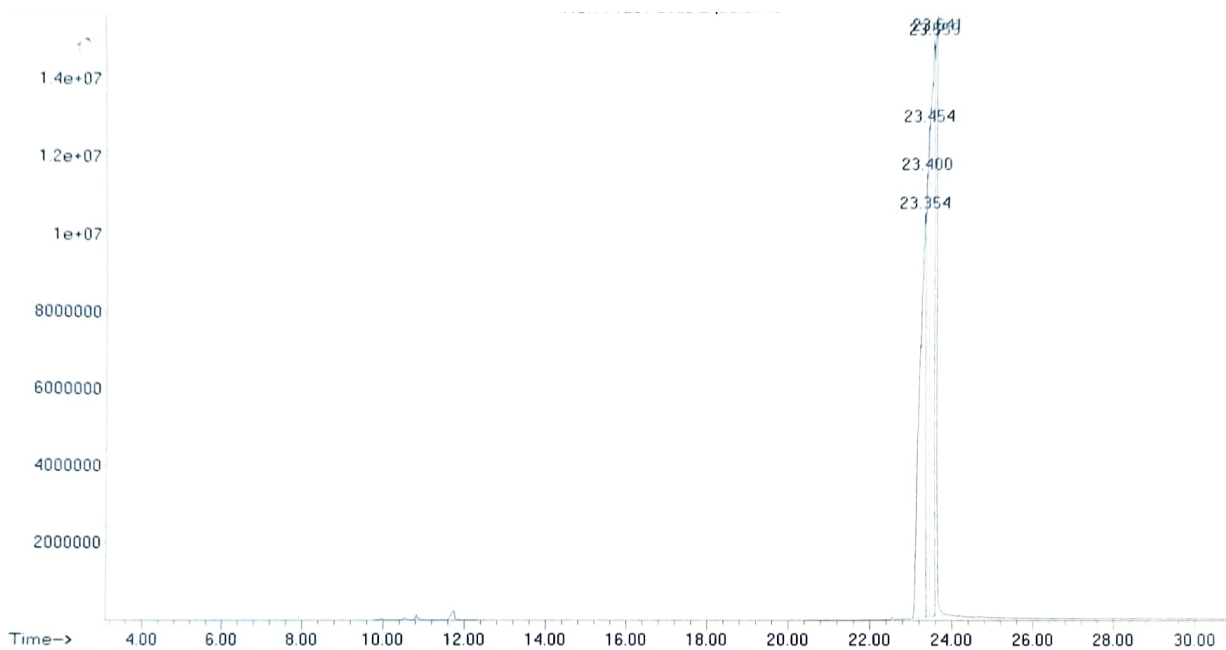


Fig. 2 : Gas Chromatogram of contraband sample

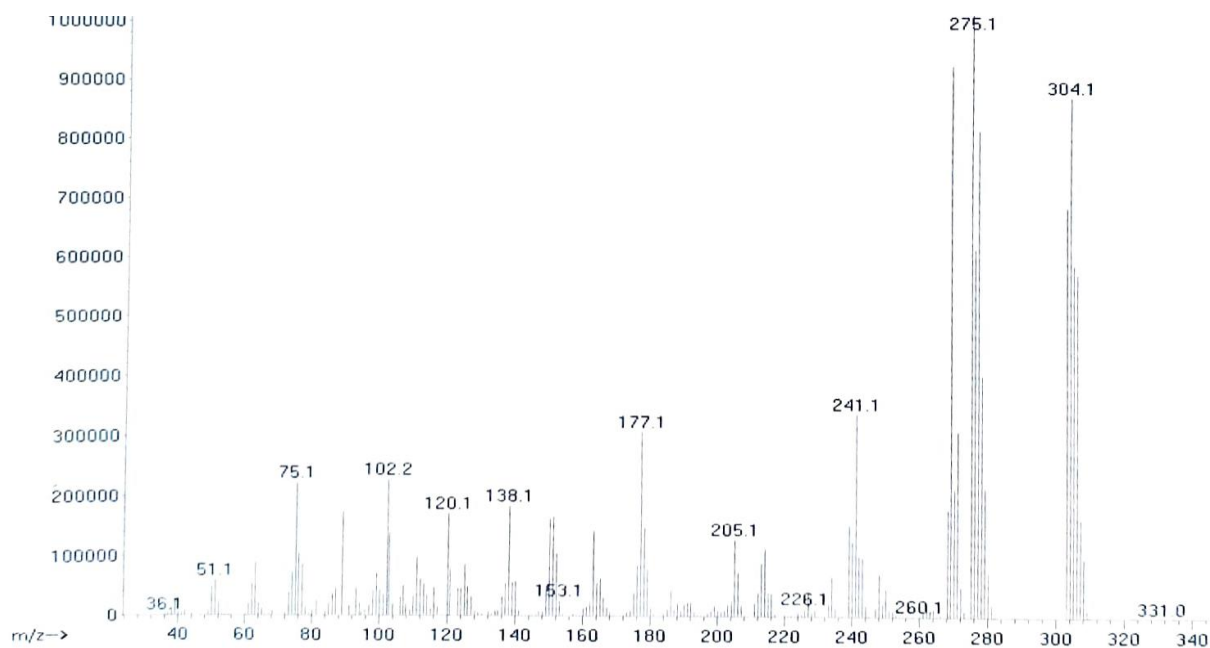


Fig. 3 : Mass spectra of contraband sample

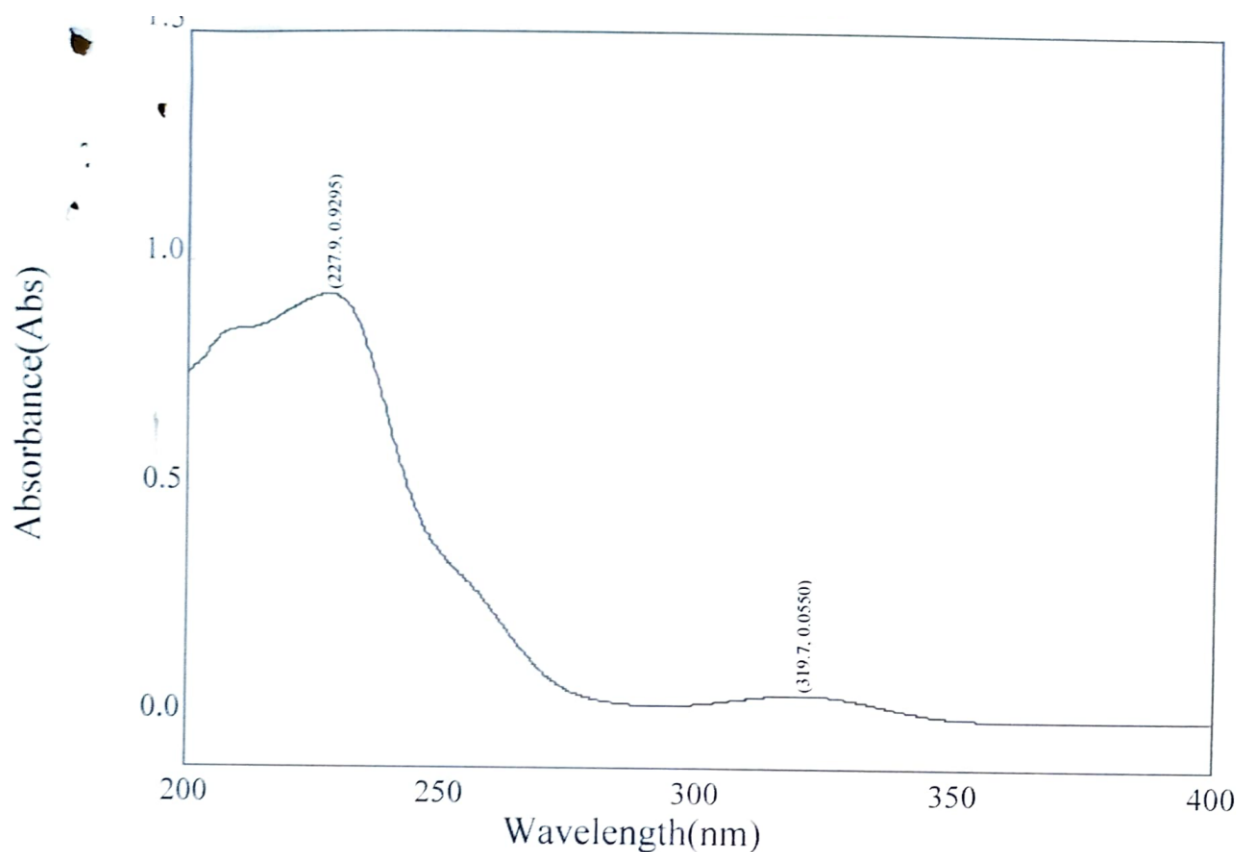


Fig. 4 : UV spectra of contraband sample

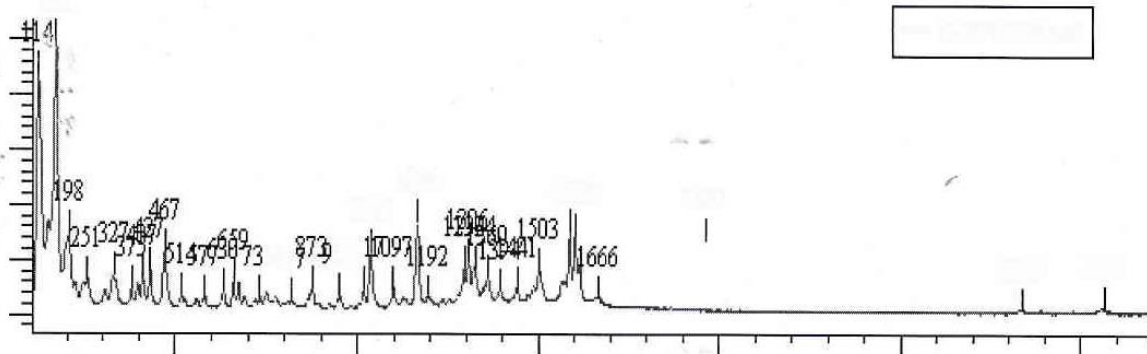


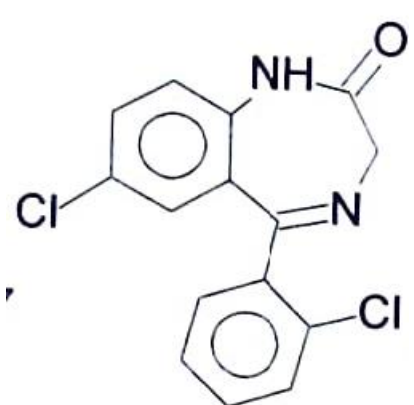
Fig. 5 : Raman spectra of contraband sample

Tables:

Table 1: Rf values of standard and samples.

Sr. No	Standard or control/ Sample	Rf
1	Std. Methaqualone	0.99
2	Std Lorazepam	0.72
3	Std Diazepam	0.98
4	Std Alprazolam	0.65
5	Std Cocaine	0.74
6	Std Ketamine	0.95
7	Std Methamphetamine	0.40
8	Sample	0.90

Table 2 : Raman spectral data of delorazepam.

Sr No	Raman shift cm-1	Assignment	Structure Found
1	427	γ atom ring	 <p style="text-align: center;">Delorazepam</p>
2	468	C-Cl stretch	
3	631	γ atom ring	
4	660	γ C=O	
5	874	γ CH	
6	1035	$-\beta$ CH	
7	1098	$-\beta$ CH	
8	1164	$-\beta$ CH	
9	1324	C=C stretch	
10	1359	C=C stretch	
11	1503	NH-def (amide II)	
12	1588	$-\text{C}=\text{C}-$ stretch	
13	1604	C=O	
14	950	γ CH	
15	515	$-\text{C}-\text{C}=\text{O}$	
16	578	$-\text{C}-\text{Cl}$ stretch	

17	1394	-C=C- Stretch	
18	731	-CH ₂	
19	1018	-βCH	
20	1295	C-NH stretch	
21	1307	- βCH	
22	1616	C=N stretch	

References-

1. Hans Maurer, Karl Pflugar, J Chromatography B: Bio Medical Sciences and Applications, 422, 85, 1987
2. K. Maudens, L. Patteet, V. Coucke, H. Neels Toxicologie Analytique et Clinique, 26(2) supplement, S21, 2014.
3. S O Chetti, M K Malve, R Krishnamurthy, The Indian Journal of Criminology and Criminalistics, XXVIII (2), 58, 2007.
4. Sandeep O Chetti, S A Shinde, M K Malve and M V Garad, Bio Chemical Science, 4(2), 73, 2015.
5. G. A. Neville, H. D. Beckstead and H. F. Shurvell, Journal Pharmaceutical Sciences , 83, (2), 143, 1994
6. Gurvinder Singh Bumbrah, Rakesh Mohan Sharma, Egypt J Forensic Sc, 6 (3), 209, 2016
7. Dipali M Atole, Hrishikesh H Rajput, Asian J Pharm Clin Res, 11(2), 59, 2018
8. Recommended Methods for the Identification and Analysis of Barbiturates and Benzodiazepines under International Control MANUAL FOR USE BY NATIONAL DRUG ANALYSIS LABORATORIES published by UNODC-2012
9. Recommended methods for the identification and analysis of methaqualone/ mecloqualone MANUAL FOR USE BY NATIONAL DRUG ANALYSIS LABORATORIES published by UNODC-2010
10. DFSS working Manual for Narcotic drugs, 2021 (New Delhi)
11. Narcotic Drugs and Psychotropic Substances Act 1985.
12. S. O Chetti, G.L Kadam and S V Ghumatkar J. Isas., 2(1), 27, 2023

From Ancient Practices to Modern Science: A Review on the Synthesis and Characterization of Ayurvedic Bhasmas

Nilima Rajurkar*, Shailesh Kantak, Babita Kale

Department of Chemistry, Savitribai Phule Pune University, Pune 411007

*Email: rnilima@rediffmail.com

Received: 7.7.2024, Revised: 19.7.2024, Accepted: 21.7.2024

Abstract

Ayurvedic Bhasma, an ancient form of Indian traditional medicine, represents a unique class of herbo-mineral formulations prepared through a meticulous process involving calcination. This review provides a comprehensive synthesis and characterization of Ayurvedic Bhasmas, focusing on its preparation methods, physicochemical properties, and characterization. The synthesis of Bhasma involves a series of Shodhana (purification), Marana (incineration), and Bhavana (soaking and drying) processes, each contributing to the transformation of raw minerals and herbs into bioavailable nanoparticles with enhanced efficacy and reduced toxicity. The review delves into the intricate processes involved in the production of various bhasmas, prepared in our laboratory as well as reports by other researchers. It also highlights modern scientific techniques used to characterize these formulations, including XRD, SEM, TEM, FTIR, AAS, NAA, DLS etc. These techniques reveal the nanoscale size, crystalline structure, and elemental composition of bhasmas, providing insights into their therapeutic potential and safety profiles.

Key words: Ayurvedic bhasma, synthesis, characterization, modern analytical techniques

1. Ayurveda and Ayurvedic Bhasma

Ayurveda, one of the oldest systems of medicine, encompasses a rich repository of traditional knowledge. Regarded as the "science of life," it has been dedicated to the healthcare of living beings since ancient times. Ayurvedic remedies, typically derived from natural sources, are employed to treat a wide array of ailments^{1,2}. Defined as a medical science focused on maintaining human health, Ayurveda offers cures and preventive measures for numerous health

conditions. Ayurvedic formulations are composed of herbal, mineral/metal, and animal substances, which are meticulously processed to achieve therapeutic efficacy³.

Ayurvedic Bhasmas stand as a cornerstone of Ayurvedic therapy, integral to the holistic healing tradition. Revered for their therapeutic properties, these finely powdered minerals and metals are employed extensively to address a myriad of ailments. Their efficacy and versatility ensure that Bhasmas remain a 'mainstay' in the realm of Ayurvedic medicine, continuously contributing to its enduring legacy.

The historical roots of bhasmas can be traced back to ancient Ayurvedic texts such as the *Charaka Samhita* and *Sushruta Samhita*, which detail the preparation methods and therapeutic applications of these substances. These texts highlight the extensive use of Bhasmas in treating a myriad of ailments ranging from digestive disorders to chronic diseases and mental health issues^{4,5}.

Modern scientific research has started to validate many of the traditional claims associated with bhasmas. Studies indicate that these preparations undergo complex chemical transformations during the incineration process, resulting in nanoparticles that possess enhanced bioavailability and therapeutic properties. For instance, swarna bhasma (gold ash) has shown promise in boosting immunity and improving cognitive functions⁶.

The preparation of bhasma is a meticulous and multi-step process, ensuring the removal of toxic elements and enhancing the medicinal attributes of the materials used. This involves repeated calcination and treatment with herbal juices, which not only detoxifies but also imbues the final product with beneficial organic compounds. The resultant ash is believed to balance the tridoshas (Vata, Pitta, and Kapha) and align the body's energies, thereby promoting overall health and well-being. These bhasmas are prepared from inorganic compounds or elements, which undergo several treatments to convert them into bio-compatible forms. During synthesis, various toxic materials are removed to minimize or eliminate any adverse effects on the body. The main advantages of bhasmas are: They are easily acceptable, palatable, fast-acting and effective in smaller dosages. They have longer shelf life without losing potency and no side effects

Improperly prepared bhasmas can produce severe adverse effects, including heavy metal poisoning, hepatotoxicity, renal toxicity, and neurotoxicity, which can sometimes be fatal. Some commercially available bhasmas have been found to contain mercury and arsenic, leading to their ban in foreign countries. Therefore, quality control, safety evaluation, and

standardization of bhasmas are of utmost importance. This can be achieved by characterizing bhasmas at various stages of preparation.

Historically, Ayurvedic physicians prepared bhasmas according to their needs. However, with the growing popularity of Ayurvedic medicines, the number of Ayurvedic pharmacies is rapidly increasing, leading to large-scale production of bhasmas in pharmaceutical houses. This commercialization has introduced several challenges, as new manufacturing appliances have not been standardized for quality. Consequently, the diverse synthetic procedures have made it difficult to determine whether bhasmas produced by different methods are identical in structure and properties, due to the lack of systematic studies from this perspective.

This review provides a comprehensive overview of research conducted on Ayurvedic Bhasmas over an extended period.

2. Synthesis of ayurvedic bhasma

Synthesis of bhasma involves number of steps. These are described below

2.1 Bhasmavidhi (The Process of Preparing Bhasma) ⁷

Shodhana (Purification): There are two types: samanya shodhana(common purification) and Vishesh Shodhana (special purification) In this process different materials used are: Sesame oil, buttermilk, cow urine, kanji, horse gram decoction, lemon juice. This treatment leads to removal of physical and chemical impurities, increased bioavailability, reduced hardness, increased brittleness and makes the material suitable for marana process

Marana (Incineration): Mercury, arsenic, sulfur and herbal products are used during marana process. It leads to alteration in structure, composition, and color, Transformation from original inorganic form to an organic, bio-acceptable form.

Chalan (Stirring): Stirring is done using an iron rod or the stem/bark of dried plants

Dhavan (Washing): In order to remove remnants of herbal products washing is done with water

Galan (Filtration): Soluble impurities are removed by filtration.

Niruthana :(absence of alloy) It is incineration of the prepared Bhasma to confirm completion of Marana.

Putana process (Heating): : The Puta is the ancient unit of heat. The obtained product is heated in fire leading to formation of bhasma.

Mardana (Trituration): Triturating the product with other substances converts it into micro-nano particles.

Bhavana (Soaking and Drying): The product is soaked in different juices and dried in a shaded place.

Amrutikaran (Detoxification): For this purpose, cow ghee and aloe vera juice are used. This will lead to removal of toxic impurities and enhancement in Bhasma purity

Sandharan (Storage): Its purpose is to maintain good quality and preserve the properties of Bhasma

Four important steps in synthesis of Bhasmas are depicted in Fig.1

2.1.1 Traditional Heating Method

Putra System: Puta is a specialized heating system used for the incineration of metals and minerals. The choice of puta depends on the type of material being processed. Different putas are used based on the quantity of fuel required. Examples mentioned in the literature include Mahaputa, Gajaputa, Kukkutputa, Varahputa, and Kapotputa. Each type of puta has a different diameter, tailored to its specific use. The intensity of heat, mode of temperature, and duration of heating vary depending on the type of puta. Putas are selected and applied for the Maran process based on the heat resistance of the material.

In the present days instead of putas electric muffle furnace is used for heating.

2.2 Ancient Ayurvedic Methods of Analysis

Classical texts have established the following parameters to ensure the proper processing of bhasma.

2.2.1 Physical Characterization:

- a. **Varna (Color):** Each bhasma has a specific color, typically white, pale, or red, depending on the initial material used. Any alteration in color indicates improper preparation.
- b. **Nisvadutam (Tasteless):** A properly prepared bhasma is tasteless when a small amount is placed on the tongue.
- c. **Nishchandravam (Lusterless):** Bhasma must be lusterless before therapeutic use. If observed in bright sunlight, the presence of luster indicates the need for further incineration.
- d. **Varitara (ability to float):** Bhasma should be light enough to float on the surface of stagnant water. Properly incinerated bhasma will float.

- e. **Unnam Test (Floating Test with Rice Grain):** This test further assesses the varitara property. A grain of rice is placed on the floating layer of bhasma. If the grain remains afloat, the bhasma is properly prepared.
- f. **Rekshapurnatvam (Fineness):** Bhasma should be finely powdered for easy absorption and assimilation. When rubbed between the thumb and index finger, it should fill the lines and crevices of the skin.
- g. **Slakshnatvam (non-rough/smooth nature):** The tactile sensation of bhasma, when touched with fingertips, should not cause irritation, ensuring it is safe for the gastrointestinal tract's mucous membrane.
- h. **Sukshmatva (Fineness):** This characteristic, indicated by the varitara and rekshapurnatvam tests, ensures that bhasma is fine enough for proper body absorption.
- i. **Anjan Sannibha (like kajal):** Properly prepared bhasma should be smooth and non-irritating to the mucous membrane.
- j. **Avami:** Bhasma should not induce nausea upon administration.

2.2.2 Chemical Characterization

a. Apurnabhavta

Apurnabhavta refers to the incapability of bhasma to retain its original metallic form. In this test, bhasma is mixed with an equal quantity of mitrapanchaka (seeds of *Abrus precatorius*, ghee, jaggery, borax, and honey). This mixture is sealed in a sharav samputa (earthen pot) and heated. The presence of lustrous particles indicates free metal, which becomes inactive after incineration.

b. Niruttha

Niruttha tests the inability of bhasma to regain its metallic form. Bhasma is mixed with a fixed weight of a silver leaf, placed in an earthen pot (sharav samputa), and heated. After cooling, the silver is weighed. An increase in the weight of the silver indicates improperly prepared Bhasma. These tests are specific to particular bhasmas. The process is not considered complete until these standards are met.

2.2.3 Methods of Physicochemical Analysis:

Delving into the essence of natural substances and their inherent properties requires precision and diligence. In this domain, the Ash Value serves as a critical measure, assessing the quality and purity of raw drugs while revealing their unique identities. Composed of inorganic elements such as phosphates, carbonates, and silicates of sodium, potassium, magnesium, and calcium, ash represents a distinctive quantitative profile for each botanical sample, facilitating precise standardization protocols.

The total ash content reflects the transformation process, where carbon and organic matter convert into ash at temperatures above 450°C. This ash contains minerals like carbonates, phosphates, silicates, and silica, providing insights into acid insolubility and water solubility—important aspects of botanical composition.

Examining further, Acid Insoluble Ash Content refines the total ash through interaction with dilute hydrochloric acid to separate water-soluble ash. This purification process not only enhances botanical analysis but also sheds light on the complex relationship between soluble salts and aqueous environments.

The Namburi Phase Spot Test (NPST)⁸, developed by Dr. Namburi Hanumantha Rao in 1970 and recognized by CCRAS, New Delhi, is an innovative method for assessing Bhasma quality. NPST utilizes chemical reactions on specialized papers to create a vivid display of color changes, capturing the dynamic nature of chemical interactions over time. Its precise measurement of sensitivity across different time intervals makes it a valuable tool for ensuring the quality of Bhasmas.

Bio-accessibility, a key factor in nutritional effectiveness, explores how nutrients are utilized within a sample, influenced by the complexities of the gastrointestinal system. Both external factors, such as the food matrix, and internal factors, like metabolic pathways, shape bio-accessibility, intertwining dietary details with physiological responses.

When it comes to estimation methods, In-vivo techniques, though time-consuming and expensive, reveal elemental bioavailability through detailed radiotracer studies, with the downside of exposure to ionizing radiation. In contrast, In-vitro techniques provide speed and cost-efficiency by mimicking digestive conditions to identify soluble and dialyzable products, offering a practical, albeit less precise, alternative to live studies. These in-vitro methods are crucial for unlocking dietary potential and pinpointing nutrient-rich supplements, demonstrating an effectiveness comparable to human and animal studies.

2.3 Modern Analytical Techniques for Characterization of Bhasma

The characterization of bhasmas involves a multidisciplinary approach, encompassing physical, chemical, and biological evaluations. This comprehensive characterization is essential for ensuring the quality, efficacy, and safety of bhasmas, thereby upholding the therapeutic principles of Ayurveda. Advances in analytical techniques continue to enhance our understanding of bhasmas, bridging traditional knowledge with modern scientific insights.

In order to characterize the bhasmas number of modern analytical techniques are available which helps to understand nature, structure, particle size, elemental content of bhasma as well as uniformity and distribution of particles in bhasmas. These are recorded in Table 2⁹⁻¹².

2.4 Synthesis/Analysis/ Characterization of Bhasmas:

A literature review reveals extensive research on commercially available bhasmas, though fewer studies focus on their synthesis and characterization. In the early 1930s, Chopra and colleagues¹³⁻¹⁷ analyzed the main constituents of bhasmas such as iron, tin, calcium, gold, and silver using classical chemical methods. Kumar et al.^{18,19} conducted elemental analysis of bhasmas using instrumental neutron activation, identifying eighteen elements. Garg et al.²⁰ employed PIXE for trace element analysis to evaluate biocompatibility in various bhasmas. Sondhi et al.^{21,22} utilized flame photometry, AAS, and ICPAES techniques to analyze bhasmas and their pharmacological effects. Krishnamurthy et al.²³ examined Lauha bhasmas from different manufacturers to understand their composition and structural characteristics. Krishnamachary et al.²⁴ studied commercially available Lauha bhasma, analyzing its morphology, structure, and chemical properties using modern techniques.

Recent advancements in analytical methods, such as spectrophotometry, flame photometry, AAS, ICP-AES, PIXE, and X-ray diffraction, have facilitated the trace elemental analysis of bhasmas. Lalla et al.²⁵ prepared, characterized, and analyzed Shankh bhasma, investigating its antacid activity. Mitra et al.²⁶ used AAS to identify twelve elements in Swarna bhasma. Prajapati et al.²⁷ assessed the safety and toxicity of tamra bhasma, lauha bhasma, and yashada bhasma, confirming no serious adverse effects. Such studies provide valuable scientific evidence to Ayurvedic practitioners and pharmaceutical R&D for better standardization of these traditional medicines.

Several researchers have synthesized bhasmas and analyzed them with modern techniques. Kumari et al.²⁸ discussed the use of modern analytical techniques such as XRD, XRF, SEM, TEM, FTIR in characterization of bhasmas along with principles of these techniques. Wijanayake et al.²⁹ explored the chemical and pharmacological properties of mica ash (Abhrak bhasma), noting structural changes during preparation. Wadekar et al.³⁰ synthesized and characterized tamra bhasma, confirming its composition matched with standard copper oxide. Gawate et al.³¹ reported physicochemical characteristics of three different brands of mandur bhasma and studied hepatoprotective activity of these. Nagarajan et al.³² characterized lead-based Naga bhasma. Pattanaik et al.³³ studied the toxicology and

antioxidant properties of tamra bhasma, showing its efficacy and safety. Jagtap et al.³⁴ evaluated tamra bhasma's quality control parameters, finding significant copper content. Gupta et al.³⁵ analyzed Yashad bhasma, revealing 98.20% zinc content. Sonkar et al.³⁶ used NPST to analyze Mandur bhasma. Pyrgiotakis et al.³⁷ compared bhasma-treated and untreated cells using Raman Spectroscopy, observing significant changes in DNA/RNA and protein molecules in treated cells.

Vasant et al.³⁸ analyzed Talaka and Naga bhasmas, identifying As_2S_3 and PbS as major constituents. They also detected minor elements like Ca, Mg, As, Sb, Al, and Fe. Dixit and Shivhare³⁹ employed modern instrumental techniques to analyze pearl and Cowrie bhasmas for minor constituents such as Mg, Ca, Fe, and Zn.

In the modern era, numerous studies have utilized advanced techniques like XRD, FTIR, AAS, ICPOES, SEM, TEM, DLS, and BET to analyze various bhasmas, including gold, silver, iron, copper, and mica. Kar et al.⁴⁰ reported synthesis and biological activity of Rajat bhasma. Formation of nanoparticles in this bhasma caused an increase in antioxidant and antimicrobial activity. Patil and Wele⁴¹ reviewed the therapeutic potential of Swarna bhasma. Recently Garg and Kumar⁴² reviewed analysis of 17 Bhasmas for their elemental content, particle distribution and toxicity. Ashvini and Kerur⁴³ analysed abhraka, mandur and godanti bhasmas of four different brands for more than 10 elements by AAS. Pandit et al.⁴⁴ evaluated the chemical and pharmacological properties of iron bhasmas, using AAS to determine 12 elements in addition to the main constituent, Fe. Buwa et al.⁴⁵ studied hepatoprotective action of abhrak bhasma in albino rats against hepatitis induced by CCl_4 while Pandit et al.⁴⁶ demonstrated shankha bhasma's anti-ulcer effects in rats.

Kantak et al.⁴⁷ analyzed copper bhasma during each stage of preparation using instrumental neutron activation analysis, finding copper concentrations of 92.89% and 59.79% after vishesh shodhana and marana, respectively. Bhowmick et al.⁴⁸ conducted physicochemical characterization of Jasada bhasma, identifying zinc as a major element next to oxygen and demonstrating the presence of nanoparticles. Singh⁴⁹ reported formation of nanoparticles of gold (size 45 nm) in the synthesized swarna bhasma.

Research has demonstrated that metals and minerals used in Ayurveda, once properly incinerated as bhasmas, can have therapeutic benefits without significant toxicity. Singh et al.⁵⁰ conducted histopathological studies on Naga bhasma, confirming its safety in rats. Wadekar

et al.³⁰ studied therapeutic properties of synthesized Tamra bhasma. Brown et al.⁵¹ characterized swarna bhasma, showing it as globular gold particles averaging 56-57 nm. These nanoparticles were found to be more effective in treating arthritis in rat models than sodium aurothiomalate.

In exploring the healthcare applications of nanomaterials, it becomes apparent that the therapeutic properties of metal-based Ayurvedic compositions may be inherently tied to their nanoscale characteristics. To harmonize the wisdom of Vedic science with contemporary scientific understanding, comprehensive physico-chemical investigations were undertaken on swarna bhasma, roudya bhasma and jasad bhasma by Amalnerkar⁵². His investigations adhered rigorously to traditional Ayurvedic preparation methods and he employed advanced analytical tools to unravel their complexities. State-of-the-art techniques such as XRD, FESEM, X-ray Photoelectron Spectroscopy (XPS), Field-Emission Transmission Electron Microscopy (FETEM), High-Resolution TEM (HRTEM), and Scanning Transmission Electron Microscopy (STEM) with High Angle Annular Dark-Field (HAADF) and Elemental Mapping were utilized. These methodologies allowed for a detailed examination of the structure, texture, morphology, and elemental/chemical composition and distribution within these metal-based formulations, thereby bridging the gap between ancient Ayurvedic knowledge and modern scientific inquiry.

Crafted from metallic raw materials, bhasmas may face challenges in complete absorption for circulation within the body. Thus, a thorough pharmacokinetic study of these bhasmas becomes crucial to accurately prescribe the appropriate dosage. Among these investigations, determining bio-accessibility stands out as a key parameter. In-vivo determination of bio-accessibility is expensive and laborious while in-vitro ones are rapid and relatively inexpensive. Katak and Rajurkar⁵³ reported bio-accessibility of abhrak naga and tamra bhasma. Tamra bhasma mixed with different anupana [material (honey and piper longum mixture, ghee and fermented juice of Aloe-vera) which increases palatibility and improves absorption] showed more bio-accessibility as compared with tamra bhasma without anupana.

In our laboratory, extensive studies have been carried out on bhasmas which comprises of synthesis and analysis of different bhasmas using traditional and modern analytical techniques. All the bhasmas were tested by traditional methods which indicated proper formation of bhasmas. Then these bhasmas were characterized by modern analytical techniques. Characterization of these bhasmas by FTIR revealed organometallic nature of the bhasmas showing several functional groups. Other important findings are listed in Table 2 along with

method of preparation and techniques applied. Some representative characterized bhasmas are shown in Figs. 2 and 3⁵⁴. Fig. 2 presents XRD of Pittal Bhasma which clearly indicated the presence of CuO with granular appearance and polycrystalline nature. SEM of Pittal bhasma is shown in Fig. 3 Examination of this figure Shows particles with change in morphology. The Bhasma prepared by Traditional Method of heating are bigger in size than that prepared by EMF heating. During synthesis of rajat bhasma, hartal and gandhaka were used in marana process. The obtained product after this process, showed presence of As. However, after Amrutikaran with lime extract this was totally removed as evidenced by EDX spectrum⁵⁹. Similarly in case of lauha bhasma synthesis, presence of Hg after marana process, done with cinnabar, was removed by amrutikaran with aloe vera extract⁵⁸.

3. Conclusion:

In summary, the synthesis and analysis of bhasma, a cornerstone of Ayurvedic medicine, bridges the rich heritage of traditional practices with the precision of modern scientific techniques. The synthesis of various bhasmas follows meticulously crafted traditional protocols, ensuring the transformation of raw materials into bioactive compounds through processes such as shodhana, marana, and amritikarana. These time-honored methods, passed down through generations, are crucial for maintaining the therapeutic efficacy and safety of bhasmas.

Characterization of bhasmas using traditional methods, including organoleptic properties, classical tests, and Ayurvedic parameters, provides an initial assessment of their quality and potency. However, integrating modern analytical techniques such as FTIR, XRD, SEM, AAS, ICP-MS enhances the understanding of their physicochemical properties and elemental composition. The amalgamation of traditional knowledge with modern analytical methodologies not only validates the ancient practices but also opens new avenues for standardization, quality control, and scientific validation of bhasmas. This comprehensive approach ensures that bhasmas can be safely and effectively integrated into contemporary therapeutic regimes, fostering global acceptance and utilization. Continued research and development in this field will further elucidate the mechanisms of action of bhasmas, optimizing their therapeutic potential and reinforcing their status as invaluable components of Ayurvedic medicine.

This review underscores the significance of integrating traditional knowledge with modern scientific validation to fully harness the therapeutic potential of Ayurvedic Bhasma. By

bridging the gap between ancient practices and contemporary science, we can pave the way for the development of novel, effective, and safe therapeutic agents derived from traditional medicines.

Figures:

General procedure for preparation of Bhasma

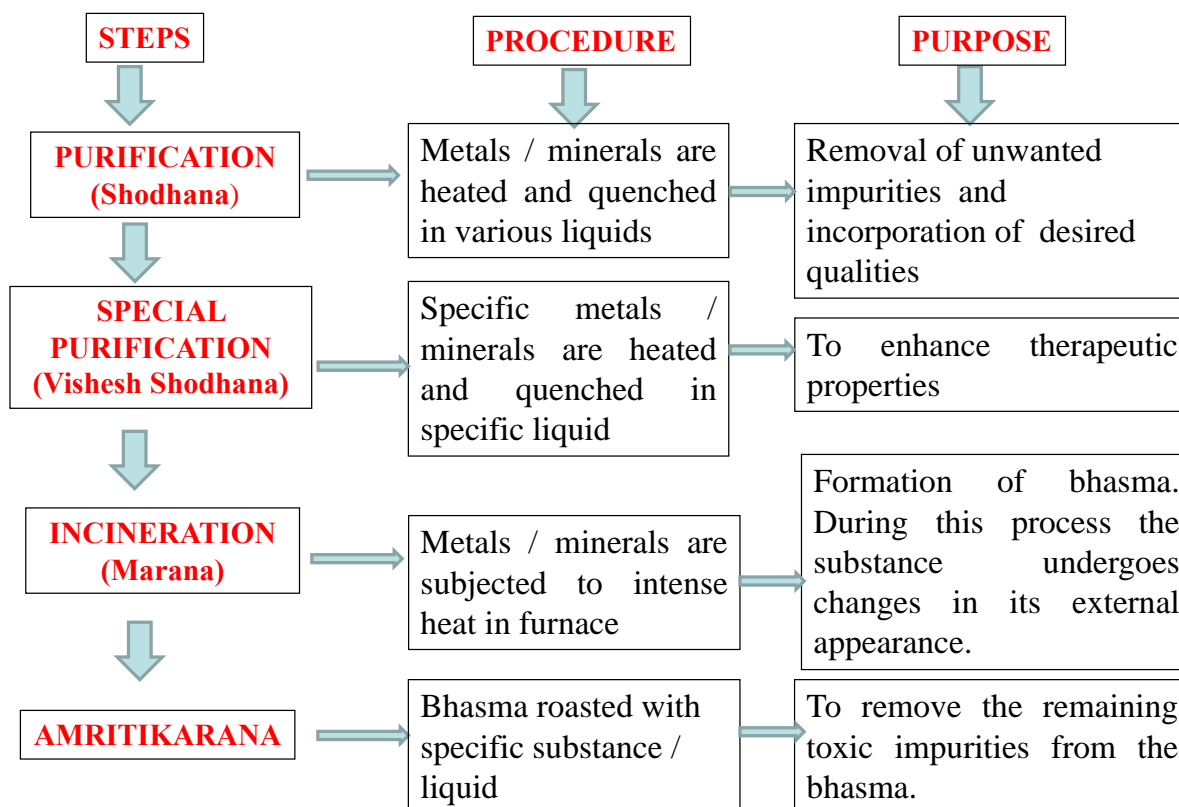


Fig. 1 General procedure for synthesis of Bhasma

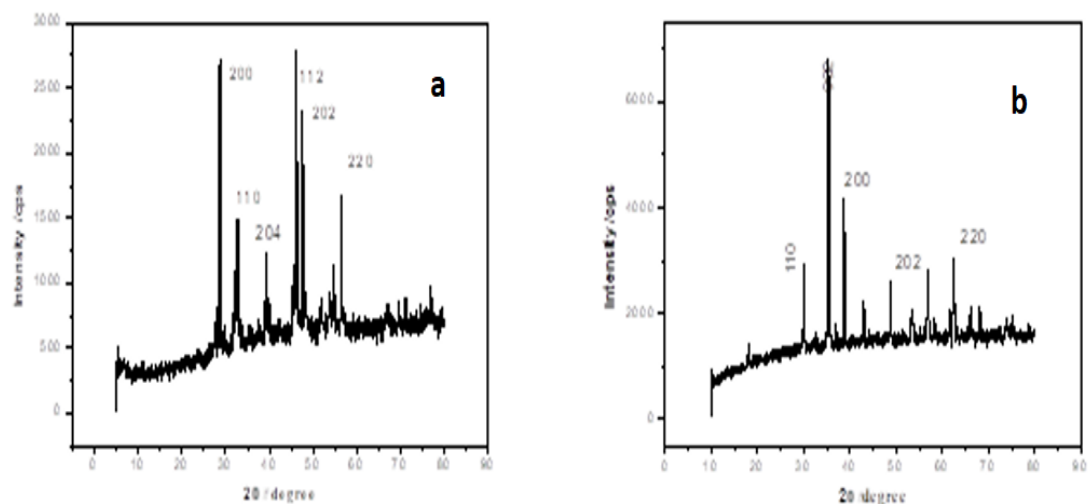


Fig.2 XRD spectra of Pittal Bhasma prepared by a) Traditional method of heating b) EMF heating

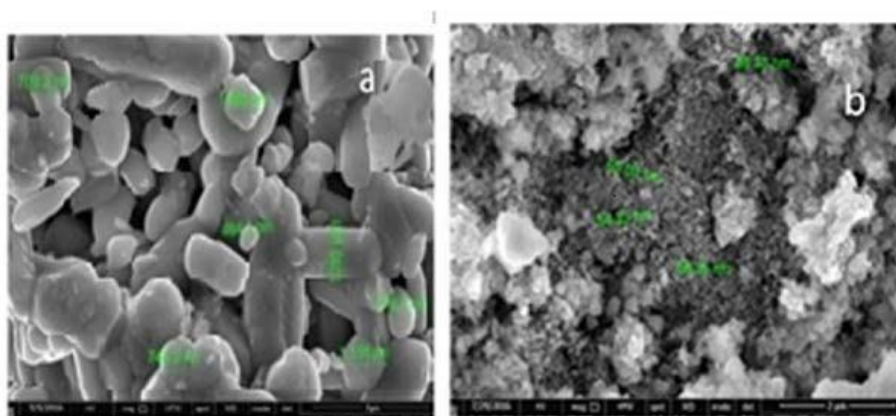


Fig.3 SEM Micrograph of Pittal Bhasma a) prepared by traditional method of heating b) prepared by EMF heating

Tables:

Table1 : Modern analytical techniques for analysis of bhasmas

Technique	Use
Fourier Transform Infrared Spectroscopy (FTIR)	Identifies characteristic functional groups and bonds present in the sample
Scanning Electron Microscopy (SEM)	Gives information about sample's surface topography and composition
Energy Dispersive X-ray Analysis (EDX)	It provides elemental analysis of areas as small as nanometers in diameter. EDX can determine elemental composition or map the lateral distribution of elements.
Transmission Electron Microscopy (TEM)	It directly measures nanoparticle size, grain size, size distribution and morphology
X-ray Diffractometry (XRD)	It identifies and characterizes unknown crystalline materials and crystallographic structure
Dynamic Light Scattering (DLS)	It measures particle size in the submicron region
Thermogravimetric Analysis (TGA)	It measures changes in physical and chemical properties as a function of temperature
Differential Thermal Analysis (DTA)	It provides data on physical and chemical changes
Inductively Coupled Plasma-Atomic Emission Spectroscopy (ICP-AES)	It is used for determining metal and non-metal elements in the sample
Atomic Absorption Spectroscopy (AAS)	It determines elemental concentration in the sample
Neutron Activation Analysis (NAA)	Useful in elemental analysis of the sample
Particle Size Distribution (PSD)	It measures particle size
Brunauer Emmett Teller (BET) analysis	It helps to determine surface area of the sample

Table 2 Synthesis and analysis of different bhasmas

Bhasma and base material used	Use	Synthesis method	Analytical methods	Important findings
Mandur ⁵⁵ It is iron based bhasma.	Generally used in the treatment of anemia, skin diseases and in poor digestion treatment.	Shodhana with Butter milk, Cow urine, Kanji, Horse gram decoction, Triphala decoction Bhavana with Triphala decoction Marana with Ardhgaja puta as well as Electric Muffle Furnace (EMF)	FTIR, SEM - EDAX, XRD	The Bhasma contains iron oxide in the form of Fe ₂ O ₃ and Fe ₃ O ₄ EDAX and SEM image clearly shows the change in morphology and decrease in particle size of the final product
Pittal ⁵⁴ It is Copper and Zinc based bhasma.	Generally used in the treatment of Liver disease, anemia, Skin diseases.	Shodhana with Butter milk, Cow urine, Kanji, Horse gram decoction, Vitex nigundo and Curcuma longa linn Bhavana with <i>Calotropis gigantean</i> Marana with Ardhagaja puta as well as EMF	XRD, FTIR, SEM, EDAX, TEM and DLS.	XRD shows the presence of CuO and granular appearance and polycrystalline nature. Particle size of Bhasma prepared by traditional method 300-750 nm while that prepared by using electric muffle furnace has 250-750 nm
Yashad ⁵⁶	Preferably used in	Shodhana with Cow milk	XRD, FTIR,	XRD shows the presence of ZnO and Zn.

<p>It is Zinc based bhasma.</p>	<p>Diabetes related diseases</p>	<p>Jarana with <i>Azardica indica</i> <i>Bhavana</i> with Orpiment purified with lime water Marana with Kukkut Puta as well as EMF</p>	<p>SEM, EDAX, TEM and DLS.</p>	<p>TEM shows the polycrystalline nature. DLS studies reveal that Bhasma prepared by EMF heating has 70 % nanoparticles in the range of 250-750nm While Traditional Method of Heating shows 200-700nm range.</p>
<p>Vanga⁵⁷ It is Tin based bhasma</p>	<p>Widely used with herbomineral formulation in Ayurveda especially for the disease related to gastrointestinal tract and genitor urinary system.</p>	<p>Shodhana with Sesame oil, Butter milk, Cow urine, Kanji, Horse gram decoction <i>Bhavana</i> with <i>Tamerandus indica lin</i> <i>Jarana</i> with <i>Aole veraTourn lin</i> Marana with Kukkuta puta as well as EMF</p>	<p>XRD, FTIR, SEM, EDAX, TEM and DLS.</p>	<p>The study confirmed the formation of organometallic compound SnO₂ The Particle size of Bhasma Prepared by traditional method of heating is 150-300 nm range and of that prepared by using electric muffle furnace has 50-100 nm range.</p>

<p>Lauha⁵⁸ It is an iron based herbo-metallic preparation and is the main constituents of iron containing formulations.</p>	<p>It is used in all chronic diseases and iron deficiency anemia.</p>	<p>Shodhana with sesame oil, butter milk, cow urine, kanji, decoction of horse gram Vishesh shodhana with Decoction of Triphala Kwatha Marana with Extract of Aloe- Vera, Cow's Urine, Decoction of Triphala Kwatha, Amritikaran with aloe vera extract</p>	<p>FTIR, XRD, TGA/DTA, SEM, PSD, EDX, BET</p>	<p>Formation of rhombohedral α-Fe₂O₃ (hematite). amount of free iron is insignificant in the bhasma. The Particle size of the bhasma ranged between 50-200nm Amrutikarna process removed Hg from the bhsama. The specific surface area of the synthesized bhasma was found to be 12.55m²/g.</p>
<p>Rajat⁵⁹ It is silver based bhasma</p>	<p>Used in eye disorders, cough, jaundice, anaemia and liver disorder</p>	<p>Shodhana with Sesame Oil, Butter Milk ,Cow's urine, Kanji, Decoction of Horse Gram, (Kulatha kwatha) Vishesh Shodhana with Jyotishmati oil Marana with Mixture of Hartal, Gandhaka and lime juice Amritikaran with lime extract</p>	<p>FTIR, XRD, TGA/DTA, SEM, PSD, EDX, BET</p>	<p>XRD analysis revealed α-Ag₂S (monoclinic) phase structure of bhasma. SEM and PSD indicated formation of nanoparticles in synthesized bhasma. Amrutikaran process was found to be effective in removal of arsenic in purified silver bhasma</p>
<p>Abhraka⁶⁰ It is prepared from abhrak or mica</p>	<p>Mainly used in the treatment of anemia and</p>	<p>Method 1 Shodhana with Cow milk</p>	<p>XRD, FTIR, SEM, EDAX, TEM and</p>	<p>XRD revealed Monoclinic KMg₃(Si₃Al)O₁₀(OH)₂ After amritikaran crystallite size increases SEM/TEM revealed:</p>

skin diseases	<p>Marana with Jaggery + juice of Ricinis communis</p> <p>Amritikaran with cow ghee</p> <p>Method 2</p> <p>Shodhana with Cow urine</p> <p>Marana with Cyprus rotundus+ calatropis procera</p> <p>Amritikaran with cow ghee</p> <p>Method 3</p> <p>Shodhana with Triphala decoction</p> <p>Marana with Turmeric powder decoction + Borax</p> <p>Amritikaran with cow ghee</p>	DLS, TGA/DTA, BET	<p>Particle range 50 nm to 1 µm.</p> <p>Few micron size (1 to 2 micron) particles seen.</p> <p>Nano size particles clustered on bigger size particles.</p> <p>Method-1 - square type particles.</p> <p>Method-2 and 3 : spherical and rod-like particles .</p> <p>DLS revealed</p> <p>Method-1 - bimodal distribution of particles with ~ 50% of particles in nanorange (50-500 nm) and remaining in micron range. micron size nature attributed to agglomeration of fused structure</p> <p>2. Method-2 and 3 show homogeneous distribution of particles with nearly 90% of particles falling in the region of 50-500 nm</p> <p>Effective diameter of bhasmas by method-1 and method-2 ranges between 500-1000 nm while that by method-3 is ~3000 nm</p>
---------------	--	-------------------	--

<p>Naga⁶¹ It is lead based bhasma</p>	<p>Used in the treatment of diabetes and skin diseases</p>	<p>Jarana Method: Vishesh Shodhana with lime water Jarana with Ash of Tamarindus indica and ash of Ficus religiosa Marana with Realgar and juice of Citrus acida Pisti Method Vishesh Shodhana with Triphala decoction Jarana amalgam of mercury Marana with Purified sulfur and juice of Citrus acida Putapaka method Vishesh Shodhana with Juice of Vitex nigundo Jarana stem of Adhatoda vesica Marana with Decoction of Adhatoda vesica</p>	<p>XRD, FTIR, SEM, EDAX, TEM and DLS, TGA/DTA , BET</p>	<p>The specific surface area of nano sized bhasmas ranges from 5 to 16 m²g⁻¹ Bhasma prepared from jarana method shows less specific surface area (~5 m²g⁻¹) than other two methods (pisti and putapaka method). The putapaka method shows maximum surface area ~16.53 m²g⁻¹. The surface area is more in bhasmas prepared by samanya shodhana process than bhasma prepared without samanya shodhana process Jarana method without samanya shodhana process ~50% particles are falling in the range of 750- 1250 nm showing homogeneous distribution of particle. Pisti method with samanya shodhana process ~ 50% of particle are in the range of 350-500 nm and that without samanya shodhana process ~ 70 % of particles are in the range of 1250-1500 nm.</p>
--	--	---	---	---

				<p>Putapaka method with samanya shodhana process ~75% of particles are in the range of 50- 750 nm while in putapaka method without samanya shodhana process ~ 60% of particles in the range 50-750 nm.</p> <p>High diameter of particles is due to agglomeration of nano particles.</p> <p>More diameter observed in bhasmas prepared without samanya shodhana process.</p>
<p>Tamra⁴⁷ It is copper based bhasma</p>	<p>Used in tumor, gland and stomach related diseases</p>	<p>Samanya Shodhana with Sesamum oil, Buttermilk, Cow urine, Kanji, Horsegram decoction Vishesh Shodhana with Cow urine Marana with Kajjali and juice of citrusacida</p>	<p>NAA</p>	<p>Copper concentration was found to vary after each stage of preparation and final concentration was found to be 59.79%</p>

References:

1. S.C. Bhargava and K.R. Reddy, Int. J. Ayurved. med., 2, 192 , 2011.
2. D. Pal, C. K. Sahu, A. Haldar , J. Adv.Pharma. Res., 5(1) 4, 2014.
3. J.T. Acharya. S. Acharya, Sushruta Samhita, commented Chaukhambha Orientalia, Seventh edn., 75, 2002.
4. V. B. Dash, Alchemy and Metallic Medicines, Concept Publishing Co., 2001.

5. B.J. Ravishankar and V. J. Shukla, African J. trad. and compliment. and alt. medicines, 4(3),319,2007.
6. C. A.Kumar, J. Ayu. Integr. Med., 8(1), 55, 2017.
7. P.G. Dileep Kumar, P. Nataraja Yadav, S. Gananadhamu, K.S. Nataraj, J. Drug Deliv.Therapeut.. 11(5):183, 2021.
8. J. Sharma, S. Rathore and H. Anitha , Int. J. Res. Trend. Innov., 7(12),4, 2022.
9. G.R. Chatwal and S.K. Anand, Himalaya publishing house, Ed.2002.
10. Transmission electron microscope (TEM), Encyclopedia Britannica., Inc.2008.
11. D. A. Skoog, F.J. Holler and S.R. Croach, Cenange India, Edn. 7., 2017.
12. U.A. Jadhao and R.K. Ingole, Int. J. Pharma., 5(10), 773, 2014,.
13. R.N. Chopra , S. Ghosh and A.T. Dutta, Ind. J. Med. Res., 22, 285, 1934.
14. R.N. Chopra , S. Ghosh and A.T. Dutta, Ind. J. Med. Res., 24, 257, 1936.
15. R.N. Chopra , S. Ghosh and A.T. Dutta, Ind. J. Med. Res., 24, 517, 1936.
16. R.N. Chopra , S. Ghosh and A.T. Dutta, Ind. J. Med. Res.,24,1137, 1937,
17. R.N. Chopra , S. Ghosh and A.T. Dutta, Ind. J. Med. Res., 24,1141, 1937.
18. A. Kumar, A.G. Nair, A.V. Reddy and A.N. Garg, Biol. Trace Element Res., 1(3) 231, 2006.
19. A. Kumar, A.G.C. Nair, A.V. R.Reddy and A.N. Garg, J. Radioanal. Nucl. Chem., 270 (1) 173, 2006.
20. R.R. Garg, N. Singh, P. N. Trehan, M.L. Garg, P. C. Mangal, F. Hennrich, H. Himmsen and H. Mommsen, Indian J. of Phys. Part B, 67(6), 581,1993.
21. S. M. Sondhi and G.K. Janani, Indian Drugs ,32, 125 ,1995.
22. S. M. Sondhi, V.K. Sharma and R.P. Verma, Indian Drugs., 33,67, 1996.
23. L.V. Krishnamurthy and R. T. Sane, Ind. Res. J. of Chem. and Environ., 5, 65, 2005.
24. B. Krishnamachary, A. Purushottam, B. Pemiah, S. Krishnaswamy , U. M. Krishnan , S. Sethuraman and R.K. Sekar, Int.J.Pharm. Pharmaceutic.Res.,4(2), 644, 2012.
25. J.K. Lalla, P.D. Hamrapurkar , P.G. Patil and H.M. Mamania , Indian Drugs., 39 ,152, 2002.
26. A. Mitra, S. Chakraborty and B. Auddy , J. Ethnopharmacology, 80 ,147, 2002.
27. P.K. Prajapati, P.K. Sarkar, S.V. Nayak, R.D. Joshi and B.S.Ravishankar, Ancient Sci. Life., 25, 1, 2006.
28. P. Kumari, Y. Yadav and K. C. Sharma, J. Tradit. Complement. Med.,5(6),122,2022.
29. A. Wijenayake, A. Pitawala , R. Bandara , C. Abayasekara, J. Ethnopharmacology., 155, 1001, 2004.
30. M. P. Wadekar , C.V. Rode , Y.N. Bendale , K.R. Patil , A. B. Gaikwad and A.A. Prabhune,

- J. Pharm. Biomed. Anal., 39, 951 , 2005.
31. R. P. Gawate, V. A. Kilor and N. P. Sapkal, *Int. J. Pharma. Pharmaceutic. Sci.*, 8(4), 327, 2016.
 32. S. Nagaranjan, B. Pemiah , U.M. Krishnan , R.K. Sekar, S. Krishaswamy and S. Sethuraman , *Int. J. of Pharm. and Pharmaceutic sci.*, 4(2), 69, 2012.
 33. N. Pattanaik, A. V. Singh, R. S. Pandey, B. K. Singh , M. Kumar, S. K. Dixit and Y. B. Tripathi , *Ind. J. of Clinical Biochem.*, 18 (2),181, 2003.
 34. C.Y. Jagtap, P. Prajapati, B. Patgiri and V. J. Shukla, *Ancient Sci. Life.*, 31(4), 164, 2012.
 35. L. N. Gupta, N. Kumar and K. D. Yadav, *Int. J. of Pharmaceut. Biol. Archives*, 5(3), 74, 2014.
 36. N. Sonkar, A. Agrawak and C.B. Jha, *Int. J. of Pharmaceutic. Res. and Biosci.*, 3(1), 229, 2014.
 37. G. Pyrgiotakis, T.K. Bhomick, K. Finton, A.K. Suresh, S. G. Kanne , J.R. Bellare , and B.M. Moudgil , *Biopolymer.*, 89 (6), 555, 2008.
 38. S.Vasanth, R.B. Bharathi, A. Mitra, S. Chakraborty and B. Auddy, *J. Ethnopharmacology.*, 80, 147, 2002.
 39. R. Dixit and G.C. Shivahare J. *Ind. Chem. Society.*, 65 , 47,1988.
 40. P. Kar, S. Banerjee, A. Chhetri, A. Sen, *J. Phytology.*, 13, 64, 2021.
 41. T. S. Patil, A. A. Wele, *Indo. Amer. J. Pharmaceutic. Sci.*, 5(1), 192, 2018.
 42. A. N. Garg and A. Kumar *J. ISAS*, 2(1), 52, 2023.
 43. A. Ashwini and B. R. Kerur, *Asian J. Pharma. Clin. Res.* 12(3), 545, 2019.
 44. S. Pandit, T.K. Biswas and P.K. Debnath, *J. Ethnopharmacology.*, 65, 149, 1999.
 45. S. Buwa, S. Patil, P. H. Kulkarni and A. Kanase, *Ind. J. Exp. Biol.*, 39(10),1022,2001.
 46. S. pandit, T.K. Sur, U. Jana, D. Bhattacharyya, P. K. Debnath, *Ind. J. Pharmacol.*, 32,378,2000.
 47. S. Kantak , T. Nesari and N. S. Rajurkar , *Proceeding of DAE-BRNS Fifth symposium on Nuclear Analytical Chemistry [NAC-V], Mumbai, India, pp.96, 2014.*
 48. T.K. Bhowmick, A. K. Suresh, S.G. Kane, A.C. Joshi and J. R. Bellare, *J. Nanoparticle Res.*, 11, 655, 2009.
 49. Y. Singh, *Int. Edu. Res. J.*, 10(4), 38, 2024.
 50. S. K. Singh, D. N. Gautam, M. Kumar, and S. B. Rai, *Ind. J. Pharm. Sci.*, 72(1), 24, 2010.
 51. C. L. Brown, G. Bushell, M. W. Whitehouse, D.S. Agarwal , S. G. Tupe, K. M. Paknikar and E.R. Tiekink , *Gold Bulletin.*, 40(3) , 245, 2007.

52. D. Amalnerkar, Azadi ka Amrit Mahotsav ISAS Webinar Series: A few Excerpts, PP 149
ISAS Publication Edited by Nilima Rajurkar, 2022.
53. S. Kantak and N. Rajurkar J. ISAS, 1(4), 25, 2023
54. B. Kale and N.S. Rajurkar , J. ISAS., 1(3) 7, 77, 2023.
55. N. Rajurkar , B. Kale and S. Kantak, Int. J. Pharmaceutic. Biol. Archives., 6(3), 21,2015.
56. B. Kale and N. S. Rajurkar, Pharma Innov. J., 7(1), 119,2018.
57. B. Kale and N. S. Rajurkar , J. Ayu. Integr.Med.,10,111, 2019.
58. 'Synthesis and characterization of iron and silver bhasma', V. B. Rathod, M.Phil. thesis,
Pune University, May 2013.
59. N.S. Rajurkar, V. Rathod and S. Kantak, Env. Observer 13,209,2013.
60. S. Kantak, N.S. Rajurkar, P. Adhyapak , J. Ayu. Integr.Med.,11 (3), 236, 2020.
61. S. Kantak and N. S. Rajurkar , J. Applicable. Chem., 6 (2), 291,2017.

Elemental Analysis of Discarded Printed Circuit Boards using Different Analytical Techniques and Recovery of Silver

Yuvaraj Kulkarni

Environmental Science Department, SPPU, Pune 411007

Email: yuvakulkarni985@gmail.com

Received: 16.6.2024, Revised: 21.7.2024, Accepted: 22.7.2024

Abstract:

The rapid advancement of technology and the demands of our consumer-driven society significantly contribute to the growing volume of e-waste generated annually. This category includes all discarded components and products from electronic and electrical equipment that are not intended for reuse. Among these, Printed Circuit Boards (PCBs) are essential elements in all electrical and electronic devices and are difficult to reuse or recycle considering the complex structure of PCB. This study focuses on analyzing PCBs for their elemental content and the recovery of precious metal, silver. Elemental concentration was analysed using Neutron Activation Analysis (NAA), nano-colorimetry, potentiometry and Atomic Absorption Spectrometry(AAS) techniques .The findings reveal that Non -metallic part in analysed PCBs is about 80-84 % while among metallic concentrations, copper concentration was found to be highest (42.88-90.80 mg/g) and that of lead lowest (0.26-0.75mg/g).The total amount of silver in three PCB samples is approximately 2 mg/g, with a recovery rate was about 66%. However, the fourth sample contains a lower total amount of silver, with a recovery rate of 52.79%.

Key words:

E-waste ,PCB, recovery of silver, NAA, Potentiometry, nano-colorimetry

Introduction:

Electronic waste (E-waste) is produced when electronic devices are disposed of once they reach the end of their operational life. The rapid advancement of technology and our consumption-oriented culture contribute significantly to the rising volume of e-waste generated annually. This category includes all discarded components and products from electronic and electrical equipment (EEE) that were not designed for reutilization¹ Printed Circuit Boards (PCBs) are essential components in all electrical and electronic devices. The materials in PCBs can be

broadly classified into Metallic Fractions and Non-metallic Fractions. From a recycling perspective, PCBs are particularly valuable due to their metal content, which is typically over 28-30%^{2,3}. PCBs are varied and intricate regarding their types, sizes, shapes, components, and compositions. Furthermore, as technology advances, the composition of PCBs continuously evolves, complicating the achievement of consistent material compositions. The intricate mix of plastics, ceramics, and metals in PCBs makes the process of liberating and separating each component highly challenging. Metals within PCBs include numerous base and rare earth metals, as well as hazardous metals^{4,5}. Traditionally, valuable metals are reclaimed from waste printed circuit boards (WPCBs) through hydrometallurgy and pyrometallurgy methods. This involves primary leaching using substances like aqua regia or various acids. Electronic waste, or electro-waste, is rich in valuable metals such as copper, silver, palladium, nickel, aluminium, zinc, gold, iron, lead, among others⁶⁻⁸.

Discarded PCBs are a treasure trove of valuable materials, interspersed with plastics and various other components. By meticulously analyzing their composition, we can innovate more efficient and effective methods to extract these precious resources. This not only minimizes our dependence on costly virgin materials but also significantly lowers the environmental impact associated with their mining and processing. Improper disposal of PCBs poses a severe threat, as they can release harmful chemicals into the environment, leading to soil and water contamination. Through detailed analysis of the materials in PCBs, researchers can identify these environmental hazards and develop strategies to mitigate them. This paves the way for safer and more sustainable recycling practices for e-waste, safeguarding both our ecosystems and public health.

Present work deals with the elemental analysis of discarded printed circuit boards and recovery of precious metal: Ag. For this different analytical techniques such as Neutron Activation Analysis, Nano-colorimetry, potentiometry and Atomic Absorption Spectrometry were used.

Experimental:

Printed circuit boards were collected from discarded computer equipments like hard disc, mother board, other cards etc. from computer hardware shop and scrap market. These were then broken down in smaller pieces of 1cm x 1cm dimension, by using pleyer. Each piece was weighed and then digested by using aqua-regia to analyse the metal concentration. By maintaining waste to aqua-regia ratio 1:1.5 for 3 h at 100 °C. After digestion solution was filtered by using Whatman filter paper no. 1. The whole solution was kept in refrigerator for

hastening crystal formation of silver chloride. Crystals were separated by filtering the solution through Whatman filter paper no.42 Filtrate was diluted to 250 ml for further experiments.

Elemental analysis of Printed circuit boards

Silver metal in PCBs was estimated by Neutron Activation Analysis (NAA) while other metals by nano-colorimetry. NAA is a non-destructive technique which was used for determination of silver in various matrices⁹⁻¹¹.

Silver estimation using NAA

The quantitative determination of Silver in PCB samples was done by NAA technique using Cf-252 neutron source available in department of chemistry, University of Pune. The neutron flux of the source determined by standard method was found to be $\sim 10^6$ n cm⁻² s⁻¹. The arrangement of facility is such a way that it gives uniform geometry of flux at the position of irradiation. One can irradiate 18 samples simultaneously, 6 in the inner core and 12 in the outer core. The flux of inner core being 1.6 times greater than the outer. It is to be noted that all the irradiations were done in the inner core.

The activity of ¹⁰⁸Ag formed after irradiation was measured using NaI (TI) detector coupled to single channel analyser. The activity at the end of the irradiation was calculated using the half-life of silver-108 and time lapse between the end of irradiation and the time of counting. The activity in terms of counts per 30 sec for silver was used to calculate amount of element in the sample.

The induced Activity is given by following equation

$$A_t = W \times L \times r \times \phi \times \sigma \times (1 - e^{-\lambda t}) / M \times 100 \quad (1)$$

Where,

W = Weight of the element, g

L = Avogadro constant, 6.022×10^{23}

ϕ = Neutron flux, n cm⁻²s⁻¹

σ = The capture cross section, cm²

r = Percentage abundance of the target, %

λ = Decay constant of the radioactive product formed, time⁻¹

t = Time of irradiation, time

A_t = Activity of the nuclide at the end of irradiation, dps

Silver was estimated by comparator method of analysis, wherein sample and standard are irradiated and counted under identical conditions.

Analysis of Aluminium, Copper, Nickel, Zinc and Lead by using Nano-colourimeter (Nano colour 500 D).

The elements Al, Cu, Ni, Zn and Pb were analysed by kits supplied by Nano colour 500 D

Determination of recovered silver from PCB and amount of silver remaining in solution

Weighed recovered silver chloride was dissolved in water by adding 2-3 drops of concentrated HNO₃. This resulted in formation of AgNO₃. For calculating the normality of silver nitrate solution, the following cell was constructed for estimation of silver:



Potentiometric titration of Recovered silver (silver nitrate) solution was carried out using KI as titrant. The amount of silver in the recovered solution was calculated by plotting EMF versus volume of AgNO₃ curve.

Remaining Silver in the solution was determined by using Atomic Absorption Spectrometer (varian spectra AA 220 AAS).

Results and Discussion:

In printed circuit boards many heavy metals are present which has potential to pollute the environment. When PCBs are not treated properly, it pollutes the environment. Therefore, it is essential to analyse the heavy metals in PCBs from which the potential hazard of PCB can be studied. In this work, PCB samples were digested using aqua regia (solid to liquid ratio 1:1.5). In the acid digestion process harmful brominated substances are evolved which were confirmed using starch iodide paper.

Analysis of non- metallic part of printed circuit boards

Fibre optics, ceramics, epoxy resin, brominated flame retardants are the non-metallic parts present in printed circuit boards which is used as base for the metallic part to be installed. In printed circuit boards 70-80 % part is non- metallic^[4]. Table 1 shows weight of PCB before and after digestion from which % of non-metallic part was calculated which is about 80-84 %.

Presence of non-metallic part in printed circuit boards depends on the use and manufacturing processes of the printed circuit boards.

Analysis of Cu, Ni, Zn, Al and Pb in PCBs by using nano-colorimeter

The elements Cu, Ni, Zn, Al and Pb in PCBs were estimated with the help of nano-colouimeter using supplied kits. The results are shown in Table 2. Following are the important findings:

- **Copper** : The concentration ranges from 45.28 mg/g to 90.8 mg/g. This is consistent with previously reported amounts of 60 mg/g to 240 mg/g ^{12,13}
- **Nickel** : The concentration ranges from 7.03 mg/g to 12.49 mg/g, which is higher than the previously reported range of 0.5 mg/g to 2 mg/g ¹³
- **Zinc** : Detected for the first time in this study, the concentration ranges from 5.65 mg/g to 9.79 mg/g. There are no previous reports on zinc concentrations in printed circuit boards.
- **Aluminium** : The concentration ranges from 10.03 mg/g to 14.28 mg/g, which falls within the previously reported range of 15 mg/g to 30.1 mg/g¹³
- **Lead** : The observed concentration ranges from 0.26 mg/g to 0.75 mg/g, significantly lower than the previously reported range of 20 mg/g to 30 mg/g ¹³.

The findings reveal that while the concentrations of copper and aluminium align with existing data, nickel levels are elevated, zinc is newly identified, and lead concentrations are significantly reduced. A detailed examination of the data shows that copper concentration in PCBs varies according to design and functionality. High-performance PCB designs necessitate higher copper concentrations. Additionally, the number of layers in a PCB impacts the overall copper levels. In contrast, nickel, zinc, and lead in PCBs are primarily present as solder alloys, with manufacturers optimizing soldering to maintain PCB quality within acceptable ranges, resulting in relatively stable concentrations of these metals across different PCBs. Aluminium is predominantly located in the capacitors of PCBs, leading to consistent concentrations across all samples.

Analysis of silver in PCBs by NAA

PCB samples were analysed by NAA wherein during irradiation of sample, (n, γ) reaction takes place on Ag present in the sample which results in ¹⁰⁸Ag. Presence of Ag was confirmed by measuring the half -life of ¹⁰⁸Ag by plotting log activity versus time curve, which was found to be 2.27 min confirming the presence of Ag in PCB. Quantitative determination of Ag in the PCB sample and in recovered Ag sample was estimated by comparator method of analysis by

irradiating and counting Ag activity of the sample and standards under identical conditions. The results are shown in Table 3

Estimation of recovered silver by Potentiometry

The recovery of silver from PCBs was determined using a potentiometric method. A graph of electromotive force (e.m.f) versus the added volume of potassium iodide (KI) is shown in Figure 2. From this curve, the amount of silver (Ag) was calculated (Table 3). The results indicate that the amount of silver recovered through potentiometric titration closely matches the results obtained from Neutron Activation Analysis.

The total amount of silver was calculated by combining the recovered silver with the remaining silver in the solution (Table 3). As illustrated in the table, the total amount of silver in the first three PCB samples is approximately 2 mg/g, with a recovery rate of about 66%. However, in the fourth sample, the total amount of silver is lower, with a recovery rate of 52.79%. Silver chloride with low solubility can't be recovered completely, hence % recovery of Ag is less. However, electrolysis method can be used further to recover remaining silver.

Conclusions:

Elemental analysis of discarded PCBs showed presence of Ag, Cu, Ni, Zn, Al and Pb amount of which varies from element to element. In printed circuit boards 80-84 % part is non-metallic. The copper and aluminium concentrations align with existing data while that of nickel concentration is found to be higher than reported. Estimation of zinc is newly reported, and lead concentration is substantially lower. Amount of precious metal, Ag, and its recovery was determined using NAA, Potentiometry and AAS techniques. The total amount of silver in the three PCB samples is approximately 2 mg/g, with a recovery rate of about 66%. However, in the fourth sample, the total amount of silver is lower, with a recovery rate of 52.79%. The results obtained by NAA and potentiometry match well with each other.

Acknowledgement:

Author is thankful to Head, Environmental Science Department and Head, Chemistry Department, SPPU for providing infrastructural facilities. He is grateful to Dr. Nilima Rajurkar, Former Head, Chemistry Department and Environmental Science Department, SPPU for her guidance and cooperation during the work.

Figures:



Fig. 1 Collected printed circuit boards scrap

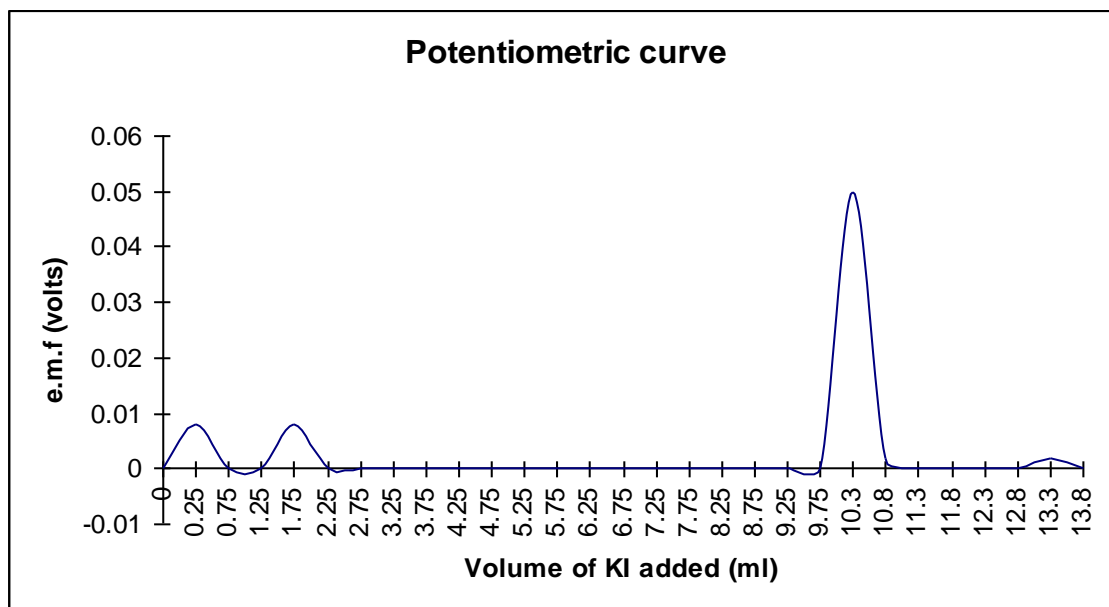


Fig. 2 E.M.F Vs added volume of KI

Tables:

Table 1 Acid digestion of Printed Circuit Boards

Printed circuit boards	Weight of PCB before digestion/g	Weight of PCB after digestion/g	Non- metallic part in PCB %
Sample 1	78.191	62.789	80.31 %
Sample 2	80.457	65.761	81.74 %
Sample 3	84.013	67.371	80.19 %
Sample 4	81.703	68.863	84.73 %

Table 2 Elemental Analysis of Printed Circuit Boards by nano-colourimeter

Printed circuit board	Concentration of metals mg/g				
	Copper	Nickel	Zinc	Aluminum	Lead
Sample 1	90.80	9.59	8.31	10.23	0.75
Sample 2	79.54	11.49	6.18	12.30	0.26
Sample 3	61.89	12.49	5.65	14.28	0.44
Sample 4	45.28	7.04	9.79	10.03	0.27

Table 3 Recovery of silver from Printed Circuit Boards

Printed circuit boards	Recovered silver mg/g (potentiometric analysis)	Recovered silver mg/g (by NAA)	Silver remaining in solution Mg/g	Total Silver mg/g	Recovery of silver %
Sample 1	1.324	1.335	0.6957	2.02	65.54
Sample 2	1.342	1.330	0.6674	2.01	66.76
Sample 3	1.384	1.370	0.613	2.04	67.84
Sample 4	0.717	0.720	0.6413	1.358	52.79

References:

1. C.P.Baldé, V.Forti .,V. Gray, R.Kuehr, P. Stegmann,The Global E-waste Monitor , United Nations University (UNU), International Telecommunication Union (ITU) & International Solid Waste Association (ISWA), Bonn/Geneva/Vienna.2017.
2. C. Eswaraiah , T.Kavitha , S.Vidyasagar , S.S.Narayanan. *Chem Eng Process: Process Intensif* ;47,565, 2008.
3. E.Y. Yazici H., Deveci. *Hydrometallurgy* ,139,30, 2013.
4. M..Jablonska-Czapla, K. Grygoyc,. *Pol. J. Environ. Stud.*,30, 1477, 2021.
5. A. Kabata-Pendias, H. Pendias, H. *Trace Elements from Soil to Human*; Springer: Berlin/Heidelberg, Germany, 2007.
6. Z.Kamberovic,M. Korac, M.Ranitovic, *Metalurgija-MJoM* , 17, 139,2011.
7. H. Li, J. Eksteen, J.E. Oraby, E. *Resour. Conserv. Recycl.* 139, 122, 2018.
8. V. Rai, D. Liu, .; D.Xia.,; Y.Jayaraman, .; J.C.P.Gabriel, *Recycling* , 6, 53,2021.
9. J. Mizera, Z.Randa,J.Kucera, J. Radioanal. Nucl. Chem. 278,599, 2008.

10. N.S.Rajurkar, A.K.Jha and R.P.Bhadane , J. Radioanal. Nucl.Chem.Lett . 186, 393, 1994.
11. V.Caramella-Crespi,U.Pisani, M.T.Ganzerli-Valentini,S. Meloni and V.Maxia, J.Radioanal. Nucl. Chem. 23,23, 1974.
12. D. Xiang, P. Mou, J. Wang, G. Duan, H. C. Zhang,. *J Adv Manuf Technol* 32, 9, 2007.
13. H. Marceloviet, A. M. Bernardes, J. Z. Ferreira, J. A. S. Tonorio, C. de Fraga Malfatti, *J. of hazardous material B*, 137, 1704, 2006.

SWASTIIK Technology for Drinking Water Treatment- “Enhancing Water Disinfection Efficacy using Fennel Oil and Hydrodynamic Cavitation”

Sanyogita N. Berde^{1,2}, Divya Dixit¹, Shilpa S. Chapadgaonkar², Vinay M. Bhandari^{1*}

¹Chemical Engineering and Process Development Division

CSIR-National Chemical Laboratory, Pune-411008, India

²Department of Biosciences and Technology

Dr. Vishwanath Karad MIT World Peace University, Pune-411038

*E-mail: vm.bhandari@ncl.res.in

Received: 17. 6.2024, Revised: 24.7.2024, Accepted: 25.7.2024

Abstract

Providing safe drinking water is of paramount importance for sustaining life. New technology, Safe Water and Sustainable Technology Initiative from Indian Knowledgebase (SWASTIIK), combining hydrodynamic cavitation and natural oils having antimicrobial properties, was evaluated for effective water disinfection using fennel seed oil for the first time. For model organism, *E. coli*, while acoustic cavitation (0.2% fennel oil) gave 100% disinfection in 10 minutes, for vortex diode cavitation device, the disinfection in 2 minutes was 70% and 99.6% at 0.5 and 1 bar ΔP respectively. Process improvement with aeration yields 100% disinfection in just 1 minute. The cost, 0.25 Rs/m³, confirmed cost-effectiveness. The hybrid approach showed highest per-pass disinfection and high cavitation yield of 236 CFU/mL/J. The oil after the treatment can be easily separated and recycled. The removal of oil was achieved using adsorption by activated carbon to restore the original taste and smell of the drinking water.

Keywords Cavitation; Disinfection; Natural oil; Process; Water treatment

Introduction

Water is essential for life on Earth, vital to many biological processes and necessary for the survival and proper operation of all living things. Its role as a transport medium enables the efficient distribution of nutrients, gases, and waste products throughout organisms^{1,2}. The scarcity of potable water is the primary cause of many ailments and disorders. A fundamental human right recognised by the United Nations is the right to access clean drinking water. However, millions of people throughout the world still do not have access to clean drinking water despite substantial advances achieved over the previous few decades. The World Health Organisation (WHO) estimates that as of 2020, around 2.2 billion people do not have access to safe drinking water. This includes 785 million people who are forced to rely on surface water sources that are frequently polluted³. Contaminated water can cause diarrheal diseases, which are responsible for an estimated 485,000 deaths each year, mostly among children under the age of five. In addition, unsafe water can lead to the spread of other waterborne diseases such as cholera, typhoid fever, and hepatitis A.⁴ The most commonly encountered coliform to signify faecal contamination is *E. coli*, which is virtually exclusively present in both animal and human faeces. Different *Escherichia coli* (*E. coli*) strains use virulence factors that have an impact on a wide range of cellular functions to cause a variety of extraintestinal and intestinal diseases⁵. Microorganisms like bacteria or pathogens can persist, multiply, and propagate in water sources, which poses serious health issues^{6,7}.

In view of the adverse effects of harmful bacteria, it is essential that appropriate methodologies be adopted for their effective removal/ elimination. Chemical disinfection methodologies involve employing chlorine-based substances (e.g. sodium hypochlorite, chlorine gas or chlorine dioxide), ozone, ultraviolet (UV) radiation, hydrogen peroxide, etc. The generation of hazardous disinfection by-products (DBPs), many of which are carcinogenic e.g. trihalomethanes and haloacetic acids, and their harmful impact on health is the main concern. Additionally, with time, some germs may become resistant to or modify chemical disinfectants, decreasing effectiveness⁸. The danger of exposure to DBP is typically thought to be outweighed by the risk of waterborne infections brought on by microorganisms⁹. Researchers are studying new water disinfection techniques due to health concerns and the rise of chlorination-resistant

pathogens¹⁰. The physical methods such as UV have limitations in terms of efficiency, scale-up or cost^{11,12}. Advanced Oxidation Processes can remove many contaminants from water and wastewater. However, some by-products generated during these processes may be more toxic than the original contaminants¹³.

Cavitation based methods have the potential to provide possible alternative to chlorination. Types of cavitation can be classified based on the mechanism that generates the cavities. These mechanisms include optic cavitation, acoustic cavitation, particle cavitation, and hydrodynamic cavitation. The cavitation mechanism, largely contributes to physico-chemical transformations via cavities generation, growth, and collapse (implosion); the implosion results in extreme temperature (10000K) and pressure (~1000-5000 atm) conditions, thereby split water thereby generating hydroxyl radicals that drive oxidation/ oxidative damage¹⁴. Thus, intensive shock waves, extreme temperature and pressure conditions and oxidative damages mainly impact the effectiveness of any cavitation process, consequently on the selection of the process type/ device type. In the field of water disinfection, cavitation reactors have been proposed as an innovative method for improving the microbiological quality of drinking water¹⁴⁻¹⁹. Furthermore, cavitation reactors have also been explored for the treatment of industrial wastewater, where they have shown potential for achieving high levels of degradation of organic pollutants²⁰⁻²¹. Adapting to stricter pollution control norms, it is necessary to study advanced cavitation processes to efficiently and economically treat complex and persistent pollutants in wastewater²². The acoustic and hydrodynamic cavitation appear to be the most promising approaches. Hydrodynamic cavitation is more efficient, easy to operate, easy to scale-up and is commonly used in industrial applications such as wastewater treatment, where it can be used to destroy organic contaminants²³. However, its potential in the water treatment is still not fully explored.

Recently, vortex flow-based cavitation reactors were reported for water disinfection²⁴. The new device was able to destroy microorganisms to a greater extent than traditional techniques. Mane and co-workers for the first time reported a new hybrid hydrodynamic process combining the traditional knowledge of Ayurveda- using natural oils, and with substantially less pressure drop compared to conventional devices like orifice^{18,19,25}. Different natural oils like eucalyptus oil, and clove oil were evaluated in combination with hydrodynamic cavitation for increased cavitation rates and the effectiveness. All the types of harmful bacteria were shown to be

completely eliminated such as gram-negative, gram-positive and also antimicrobial-resistant bacteria (AMR) and difficult to treat, opportunistic pathogens¹⁹. The new technology was named as SWASTIHK- Safe Water and Sustainable Technology Initiative from Indian Knowledgebase. The process was further improved by Dixit et al. using different newer natural oils such as Ajwain, thyme, oregano, peppermint, harsingar, cinnamon leaf, and black pepper oil etc. and for different formats and molecular docking studies²⁶.

The new technology, SWASTIHK, has potential to offer the most promising alternative to the existing chemical methods simultaneously eliminating the disadvantages of harmful DBP formations apart from being simple and cost effective. It is, however, imperative to evaluate best possible alternatives in Ayurvedic natural oils that not only intensify the process for instant disinfection, but also possibly help in generating quality drinking water without taste problems or odour or even for possible health benefits. Studies have provided valuable insights into the efficacy, safety, and potential health benefits of essential oil compounds in water treatment, suggesting their application in SWASTIHK technology for disinfection purposes²⁷.

It is therefore the objective of this study to further extend the scope and horizon of the methodology by newer investigations on natural oils and process validation for complete elimination of *E. coli*, a Gram-negative, facultative anaerobic bacterium. Use of Fennel oil was considered for the study in this regard for investigating acoustic cavitation and hydrodynamic cavitation using vortex diode, since Fennel oil has trans-anethole (80.8%) and estragole (9.6%), which are known to have antibacterial characteristics^{28,29}. The essential oil obtained from fennel seeds has potent antibacterial properties and could be used as a natural alternative to synthetic antibacterial agents and its use in SWASTIHK can be potentially more attractive.

Material and methods

Materials

Bacterial strain of *Escherichia coli* (ATCC-8739) was obtained from NCIM- National Collection of Industrial Microorganism at CSIR- National Chemical Laboratory, Pune, Bharat. Nutrient Broth (Himedia Nutrient HiVeg broth) was used as the cultures growth medium and Nutrient agar (Himedia) was used to plate the culture and get total bacterial count of the *E. coli* present in the sample. A 100% pure therapeutic grade natural fennel oil, derived from the seeds of *Foeniculum vulgare Mill*, was obtained from local sources. The oil was acquired in its pure

form and was used without any further processing or alterations, ensuring its original chemical composition and properties remained intact.

Measurement of disinfection activity

The bacterial strain was inoculated in 100 mL Nutrient Broth (Himedia Nutrient HiVeg broth) which was further incubated at 37°C overnight at 200 rpm in an incubator-shaker. As it is more challenging to eradicate bacterial colonies that grow robustly as opposed to saturation or death phase, robust growth phase was established by incubating bacteria overnight. To achieve a final concentration of 10^4 - 10^5 CFU/mL, the known bacterial culture concentration was prepared using distilled water for acoustic and hydrodynamic cavitation studies.

The system's viable bacterial population was determined using the plate count method. At regular intervals starting from 1 minute, samples were collected from the cavitation experiments and 100µL was then plated onto a sterile petri plate containing Nutrient agar medium. The colonies were measured by Eq. 1, colony forming units per millilitre (CFU/ml) after the plates were incubated at 37°C for 24 hours.

$$\frac{CFU}{ml} = \frac{\text{Number of colonies on N.Agar plate}}{\text{volume plated (mL)}} \times \text{dilution factor} \quad (1)$$

The difference in the starting and final concentrations was used to compute the percentage disinfection.

Acoustic Cavitation

A UCP-20 Sonication Unit was employed to induce acoustic cavitation using a frequency of 40 kHz and a power level of 500 W. Four flasks, each containing 200 mL contaminated water samples with known levels of microorganisms were studied for a duration of 15 minutes. The effect of concentration of fennel oil was studied for 0% (no oil), 0.05%, 0.1%, and 0.2%. The samples were collected at specific time intervals during the operation.

Hydrodynamic Cavitation

A vortex flow-based hydrodynamic cavitation was employed using a vortex diode as a cavitating device (MOC- Aluminium, chamber diameter of 66 mm and capacity of 1 m³/h). The experimental set-up consists of a high-pressure multistage centrifugal pump, a 50 L

volume water storage tank, cavitating devices, temperature control using a JULABO Chilling system (Model FL 1701), and pressure and flow controls/indicators. The details of the set-up are well reported in the previous studies¹⁸.

A typical volume of 20 litres of contaminated water, with a known concentration of *E. coli* bacteria was added to the tank. The water was pumped through vortex diode using specified pressure and specified experimental conditions. Three different pressure drop levels: 0.5 bar, 1 bar, and 1.5 bar were evaluated for the pressure effect. Similarly, the concentration of fennel oil was varied at three different levels: 0.05%, 0.1%, and 0.2% (v/V). The samples were collected at predetermined time intervals and analysed for extent of disinfection under different conditions. Process intensification was studied using aeration at an optimized pressure drop of 1 bar for two different conditions: without the addition of fennel oil and with the addition of 0.1% fennel oil.

Elimination of taste and smell

The taste and odour removal studies were carried out using adsorption technique and NORIT as an adsorbent. A packed column was assembled, starting with a layer of glass wool at the bottom, followed by activated norit carbon above it. The treated water samples were collected at different time intervals.

Results and discussion

The efficacy of the different methodologies can be best evaluated using *Escherichia coli* (*E. coli*), a standard model organism, frequently used as an indicator organism in microbiology studies as it indicates faecal pollution / related health problems corresponding to its presence in water³⁰⁻³². The disinfection was studied using both, acoustic and hydrodynamic cavitation methods; with and without addition of the fennel oil at different operating conditions and using process intensification with aeration in hydrodynamic cavitation. The results are discussed below.

Acoustic Cavitation

The results on disinfection using fennel oil and acoustic cavitation are shown in Fig 1. It is evident that the concentration of the fennel oil has significant effect of the extent of disinfection and disinfection efficiency increase with the increase in the concentration of fennel oil.

Compared to only ~20% disinfection using only acoustic cavitation, a complete disinfection, 100% removal, was achieved using 0.2% fennel oil solution within 10 minutes (Fig 1. (b)). The results of Fig. 1 depicting complete elimination of the harmful bacteria are important in highlighting the efficacy of fennel oil in disinfection by the process of acoustic cavitation, especially for a smaller scale of operation. The huge enhancement in the rate constant values and also enhanced synergy in the combination of acoustic cavitation and the fennel oil (Table-1) also confirms the utility of using fennel oil in this regard.

Hydrodynamic Cavitation- Effect of Pressure

The pressure drop across the cavitating device is one of the most important parameters in any hydrodynamic cavitation process from energy utilization point of view. There are many different designs in cavitating devices, the simplest being orifice with a single hole and is based on using linear flow and obstruction in the path for sudden pressure drop. A vortex flow based device employs swirling/ vortex for generating the sudden pressure drop, requiring a specific design of the chamber for the specified flow³³. Vortex diodes as reactors and effluent treatment devices. A vortex diode used in the present study requires significantly lower pressure drop compared to orifice and also was found to be more efficient with only pressure drop of 0.48 bar as point of cavitation inception²⁰. The experiments were carried out using the pressure drop of 0.5, 1.0 and 1.5 bar to ensure the process in the cavitating regime.

The results of pressure variation, without addition of natural oil, are shown in Fig 2. Lower pressure drop of 0.5 bar yields a disinfection of 65%, while a slightly lower value of 61% was achieved at a pressure drop of 1.5 bar in 60 mins. Interestingly, at a pressure drop of 1 bar, a high efficiency, 82% disinfection was observed. Thus, the optimum pressure drop conditions can be seen as 1.0 bar pressure drop, under the conditions of no oil addition.

Hybrid Hydrodynamic Cavitation- Effect of Fennel Oil

The results of hybrid cavitation process using fennel oil and acoustic cavitation were excellent giving 100% disinfection in 10 minutes for 0.2% oil addition. Thus, it would be prudent to evaluate efficacy of hydrodynamic cavitation in this regard as significant improvement can be expected. By using the pressure drop conditions of ΔP 0.5 bar and 1.0 bar, three different concentrations of fennel oil were investigated: 0.05%, 0.1%, and 0.2%. The results are shown in Figs. 3 and 4.

As expected, due to the intense conditions of hydrodynamic cavitation, the disinfection is achieved in remarkably short time intervals and oil addition provides tremendous impetus. A concentration of 0.2% fennel oil resulted in > 99.6% removal of the target microorganisms within just 1 minute of operation compared to ~10 minutes in acoustic cavitation. The concentration of 0.1% fennel oil showed 70% reduction in microbial load within 1min implying that critical concentration of the natural oil is essential for achieving 100% disinfection and also that appropriate hybrid combination is essential. The results also highlight the importance of the methodology since many earlier investigators failed to accomplish 100% disinfection using any of the cavitation format-acoustic or hydrodynamic, using any of the cavitating device with the efficiency comparable to this work. Further, the rapid disinfection underlines the effectiveness of fennel oil as a powerful antimicrobial agent.

The progress of disinfection shows an interesting trend with respect to both pressures drop and for oil concentration. A disinfection of 82% within 60 minutes at a pressure drop of 1 bar can be altered to ~90% by the addition of fennel oil (0.05%) in just 10 minutes. With 0.1% oil, the disinfection is 92% in 10 min and with 0.2% oil, > 99% in just 2 minutes. These results clearly show that the fennel oil, especially at higher doses, significantly enhances the disinfection process. The results (Fig. 4) indicate 1 bar pressure drop and 0.2% oil concentration to be most effective in achieving 100% disinfection.

Hydrodynamic Cavitation- Effect of Fennel Oil- Process Intensification

As mentioned earlier, aeration is one of the simplest forms of process intensifications which can contribute to increasing number and quality of the cavities consequently enhancing the performance of the hydrodynamic cavitation process. In the present study, a simple air pump was used to bubble air by inserting tube in the storage tank containing water. An optimized pressure drop of 1 bar was used to compare the results. The results of process intensification in the form of aeration are shown in Fig 5.

It is interesting to note the progression in achieving the enhancement in disinfection: The aeration has marginal impact in the initial progress though both HC and HC+aeration yield 80 % disinfection in 60 minutes, but no oil addition, clearly and this gets further enhanced to 100% disinfection for the combination of HC + aeration + fennel oil (0.1%), at the same ΔP of 1 bar,

highlighting the aeration impact in the hybrid process (SWASTIHK). Most importantly, the time required for the complete disinfection is just 1 min compared to the 60 minutes of HC that too with limited 80% disinfection. Thus, from the results of Fig. 5, it is evident that a complete elimination of harmful bacteria, *E. coli*, can be accomplished instantly using mild operating conditions (ΔP 1 bar, HC+aeration+0.1% fennel oil).

Per-Pass Disinfection

The enhancement in the rates of disinfection can be quantified for different process formats using the rate model- per pass disinfection^{18,25}. The per-pass disinfection factor physically describes the disinfection behaviour in hydrodynamic cavitation systems and provides useful information on the extent of disinfection per cycle, number of passes for achieving the desired effect and therefore also on the effectiveness of the process apart from cost of the process. The following rate equations were used:

The effective disinfection rate constant (k), measured in s^{-1} , is determined in the following manner in the conventional model:

$$k = \ln \left(\frac{C_0/C}{t} \right) \quad (2)$$

In this case, C_0 and C stand for the initial and current concentrations of bacteria, both expressed in CFU/mL, at any given time t .

The effective rate constant (k), also expressed as s^{-1} , in the per-pass disinfection model of hydrodynamic cavitation is defined as follows:

$$k = \frac{\varphi n}{t} = \frac{\varphi}{\tau} \quad (3)$$

where, n is the number of passes, and φ the per-pass disinfection factor, which quantifies the importance of any cavitating device.

The per-pass disinfection factor (φ) can be calculated as:

$$\varphi = -\ln \left(\frac{C/C_0}{n} \right) \quad (4)$$

An important factor used in cost estimates is the number of passes (n), since a lower value of n directly relates to a lower cost of the disinfection procedure. The following equation can be used to calculate the number of passes.

$$n = \frac{Qt}{V} \quad (5)$$

Where, Q is the flow rate, t is time, and V is the volume treated. By using this model, it is possible to determine the per-pass disinfection factor and the effective rate constant, which facilitate correct comprehension and analysis of the disinfection process. The results of using the model are presented in Table-1 and in Fig. 6.

The order of magnitude enhancements in the use of natural oil and the hybrid cavitation process is clearly evident from the results. At ΔP 1 bar, concentrations of 0.05%, 0.1%, and 0.2% of fennel oil requires 6 passes each. It should be noted that the effective oil concentrations in this SWASTIHK process depends on the nature of the oil and also on the nature of the intensification, if any.

The combination of aeration, 0.1% fennel oil, and ΔP 1 bar results in the greatest improvement. The number of passes in this situation drops considerably to 0.6, showing practically instant disinfection within single pass.

Plausible Mechanism for Disinfection

The mechanism of SWASTIHK process has been well discussed in the recent times. However, specific action of natural oils having antimicrobial activity depends on the inherent constituents, often many, that participate in damaging the cell structure along with cavitation attributes. The high efficiency using fennel oil, therefore, can be attributed to the content of oil which includes phenols, terpenes, bioactive compounds such as anethole, fenchone, and limonene and other antibacterial compounds. These damage/destroy microbial cell membranes, leading to cell destabilisation and eventual death^{34,35}. The lipophilic compounds in fennel oil can interact with the lipid bilayer of the cell membrane, leading to its destabilization and subsequent leakage of cellular contents. Some components of fennel oil, such as anethole, have been shown to inhibit specific bacterial enzymes. This inhibition can interfere with essential metabolic pathways or processes within *E. coli* cells, ultimately leading to cell death. The oil also contains compounds that can generate reactive oxygen species (ROS) when exposed to bacterial cells. ROS can cause oxidative damage to cellular components, including DNA, proteins, and lipids, thereby impairing vital cellular functions and leading to cell death. Fennel oil also prevents the growth of different microbes by interfering with their enzyme and

metabolic systems. Additionally, the antioxidants in fennel oil cause germs to experience oxidative stress, which damages vital biological components and causes inactivation. However, in order to maximise the efficacy of fennel oil as a disinfectant, it is crucial to take into account variables like concentration, exposure period, and the nature of specific bacteria targeted³⁶⁻³⁷.

The effects of the oil and cavitation can be seen in Figs. 7 and 8. Through intense shock waves, shear forces, and high temperatures and pressures generated during bubble collapse, hydrodynamic cavitation can physically disrupt the cell membranes of *E. coli*, leading to cell death. The localized hotspots and high-pressure regions are generated during the implosion can induce thermal and mechanical stresses on the *E. coli* cells, potentially damaging their cellular components and disrupting vital cellular processes. Hydrodynamic cavitation produces reactive species, such as hydroxyl radicals ($\cdot\text{OH}$), which have strong oxidizing properties and contribute in oxidising the biomolecules within *E. coli* cells leading to cellular damage and inactivation.

Removal of Taste and Smell pertaining to the Natural oils

The addition of oil imparts odour and taste, many a times not pleasant, and therefore not desirable for the drinking water purpose. The oil-water separation is easy and can be accomplished by a number of techniques, the layer separation being the simplest one. In this work, we have used adsorption technique similar to that used in the household water purification systems. The water was passed through the bed of adsorbent- Norit activated carbon to remove the flavour and smell of fennel oil. The treated water after the adsorption step was found to normal drinking water without any taste of oil or odour.

Energy and Cost Calculation

The cavitation yield per volume treated (CFU/mL/J) can be obtained by Eq. 7

$$\frac{\text{cavitation yield}}{\text{volume treated}} = \frac{(c_0 - c)}{(\Delta P \times Q \times t)} \quad (7)$$

The cavitation yield represents the efficiency of the different processes and the order of magnitude higher values for the combination of HC+aeration+Fennel oil validates the efficacy of the suggested process over the conventional one (Fig 9). To calculate the cost of treatment per cubic meter of water using the equation provided, the values for the number of passes (n),

pressure drop (ΔP), power consumption (P), and pump efficiency (η) are needed. Given that the flow rate (Q) for a vortex diode measured at a pressure drop of $\Delta P = 1$ bar is 710 LPH (litres per hour) and the volume treated is 20 L (litres), the number of passes, n can be obtained.

The cost of treatment can be calculated by Eq. 8

$$\frac{\text{cost of treatment}}{\text{m}^3 \text{ of water}} = \frac{n\Delta P P_E}{36\eta} \quad (8)$$

Considering the cost of electricity (P_E) at 10 Rs/kWh and a pump efficiency (η) of 0.66, the cost of treatment per cubic meter of water can be calculated. At 0.2% fennel oil and without aeration, corresponding to 100% removal of bacteria in 2 minutes, the cost of treatment was just 0.498 Rs/m³, with high cavitation yield of 117.4 CFU/mL/J, compared to 2.5 Rs/m³ for 0.1% oil. The cost is drastically reduced by 10 times with process intensification using aeration for HC + aeration + oil, resulting in 0.25 Rs/m³. In general, the cost of the chlorination process is the lowest among all the methods (~0.32 Rs/m³), while the costs for physical and physicochemical methods range from 80 to 650 Rs/m³ ²⁶. The overall operating cost of the present disinfection process is expected to be comparable to or even lower than that of chlorination without having any disinfection by-products. Additionally, the oil can be recycled and used again, making the cost of fennel oil negligible. These values indicate that a particular treatment combination needs to be explored for achieving instant disinfection. The cost of 0.25 Rs/m³, and the yield of 236.4 CFU/mL/J signifies a high effectiveness in reducing the microbial load for the drinking water treatment and the techno-economic viability of the process.

Conclusions

The present study introduces a novel application of fennel seed oil in the hybrid cavitation process-SWASTIHK, offering promising consequences for water disinfection. The main findings of this innovative green hybrid cavitation technology are as follows:

1. Acoustic Cavitation: Complete disinfection of *E. coli* was achieved within 10 minutes using a 0.2% fennel oil solution.
2. Hydrodynamic Cavitation using vortex diode yields close to 100% disinfection within 2 minutes for 0.2% oil concentration and for 0.5 bar pressure drop. Increasing the pressure drop to 1 bar, reduces the oil dose.
3. Process Intensification by aeration and for pressure drop of 1 bar and 0.1% fennel oil concentration yielded complete disinfection (100%) within 1 minute.

4. The process using fennel seed oil in the hybrid cavitation process, at a concentration of 0.1%, resulted in significantly lower costs (0.25 Rs/m³).

Overall, the study demonstrated the potential of SWASTIHK process of hybrid hydrodynamic cavitation using fennel seed oil for rapid and efficient disinfection of *E. coli*, highlighting its potential for large-scale applications.

Statements and Declarations-

Funding Sources- Acknowledgement

The author-VMB wishes to acknowledge the financial support from Water Innovation Center-Technology, Research and Education (**WICTRE**) (**DST/TM/WTI/WIC/2K17/100(G)**), of Department of Science and technology, Ministry of Science and Technology, India and also financial support from Council of Scientific and Industrial Research (CSIR), Government of India (**MLP102326**). Divya Dixit would like to acknowledge fellowship of Department of Science and technology, Ministry of Science and Technology India.

Figures:

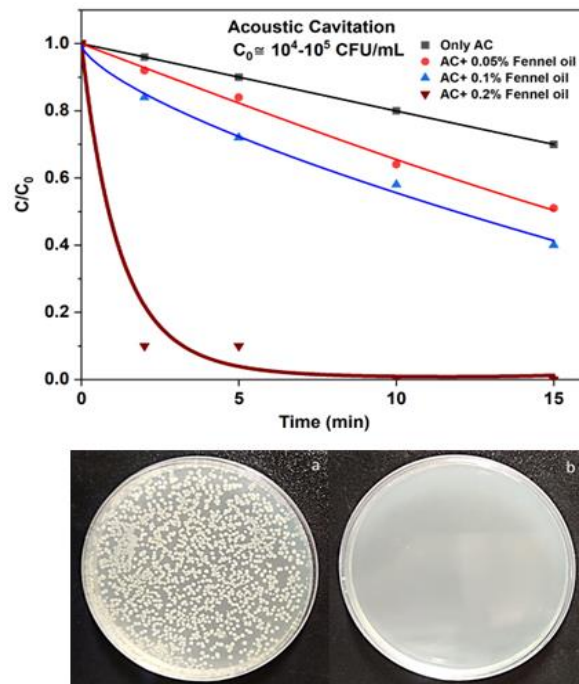


Fig. 1: Effect of fennel oil in acoustic cavitation, (a) 0 min (b) 10 min (0.2% fennel oil)

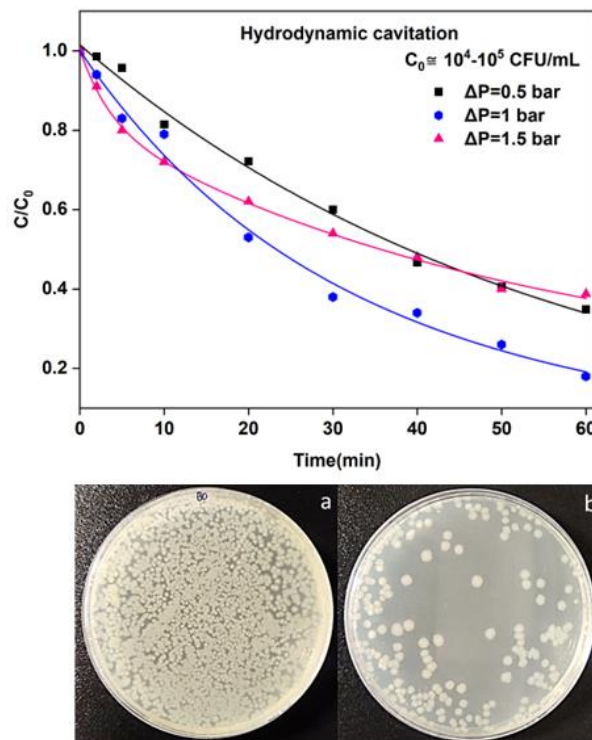


Fig. 2: Effect of pressure on disinfection using hydrodynamic cavitation (a) 0 min (b) 60 min (ΔP 1 bar)

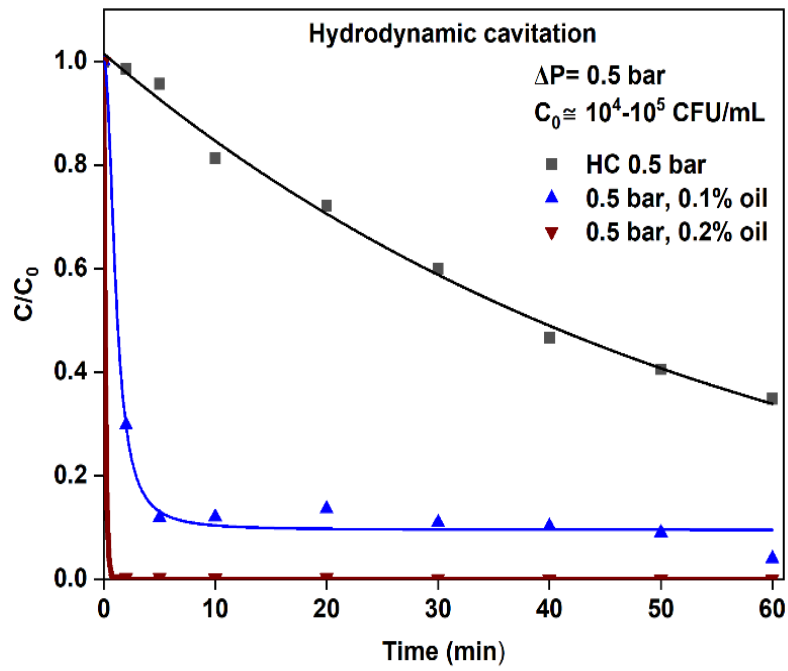


Fig. 3: Effect of varied fennel oil concentration at ΔP 0.5 bar

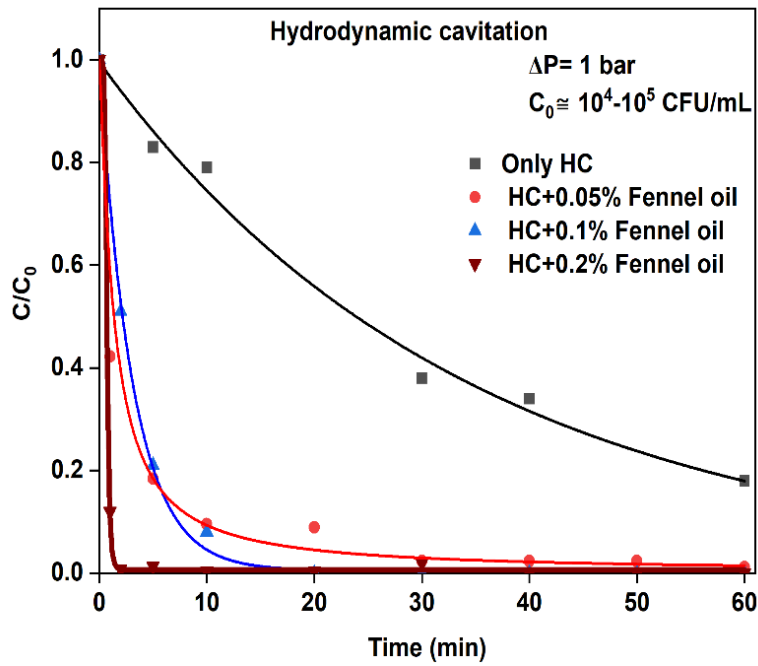


Fig. 4: Effect of fennel oil concentration at ΔP 1 bar

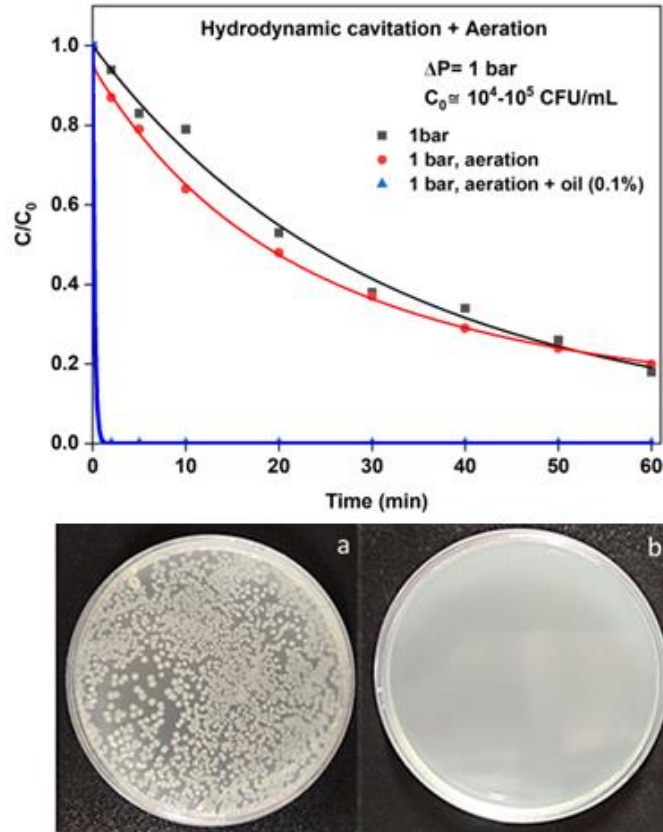


Fig. 5: Effect of aeration in hybrid methodology, (a) 0 min (b) 1 min (ΔP 1 bar, 0.1% fennel oil)

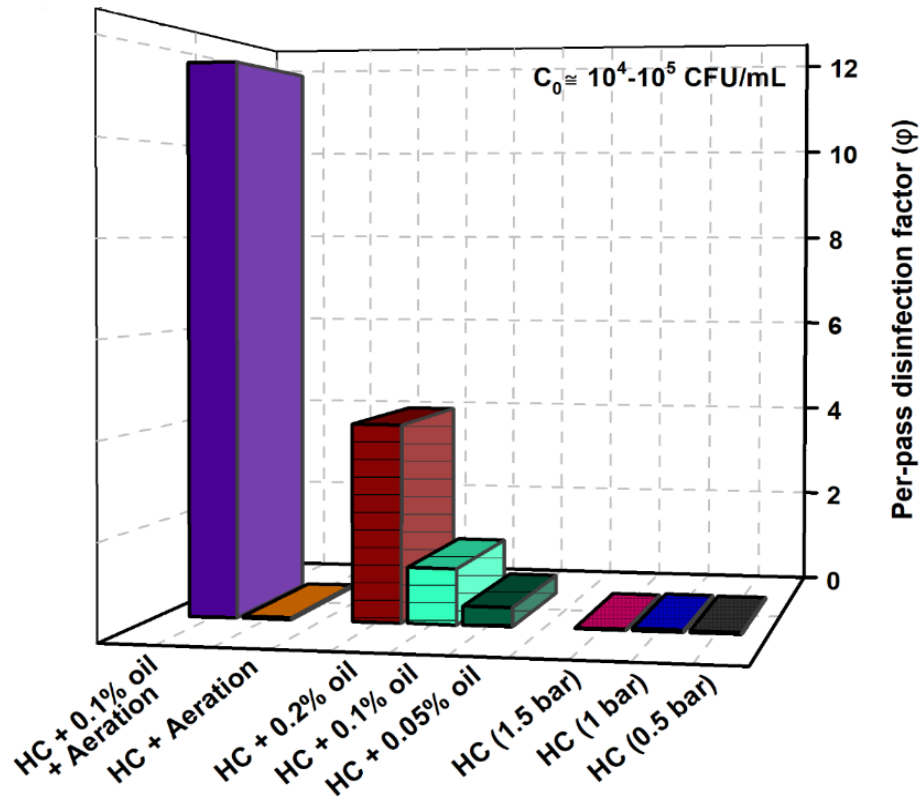
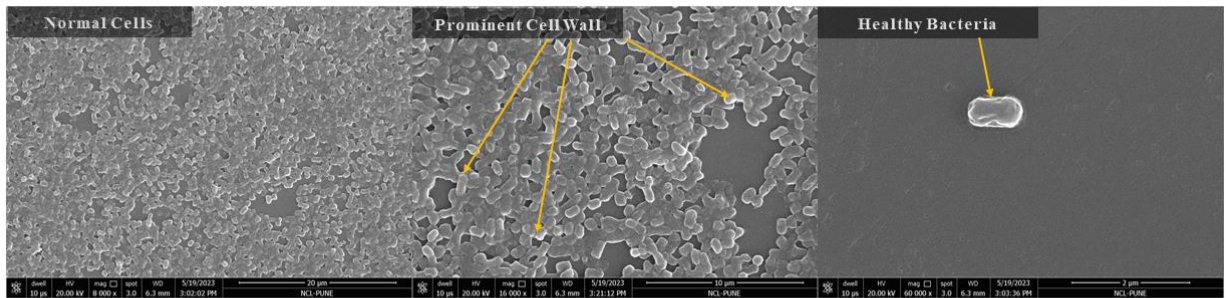


Fig. 6: Per-pass Disinfection

FE-SEM Images of *E. coli* before treatment



FE-SEM Images of *E. coli* after treatment

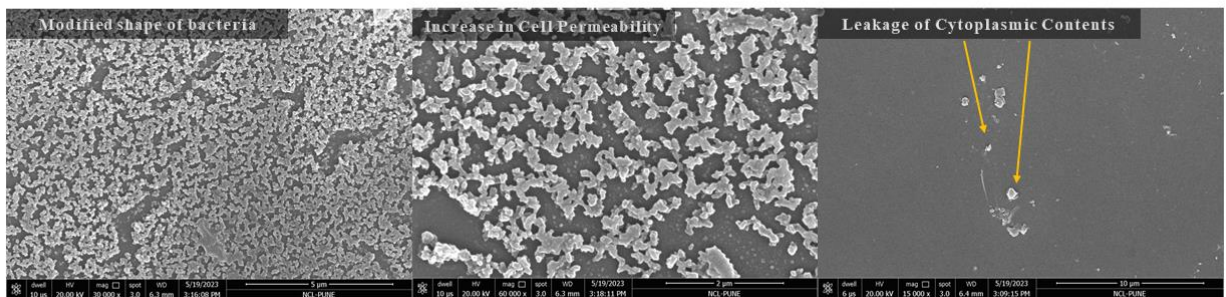


Fig 7: FE-SEM images of the effect of fennel oil on *E. coli*.

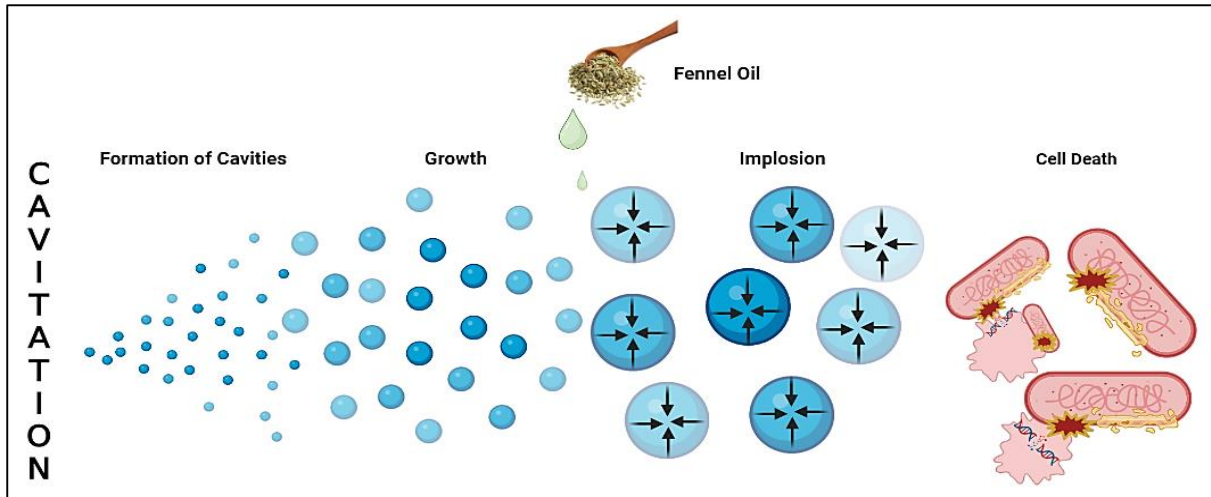


Fig 8: The effect of hydrodynamic cavitation and fennel oil on *E. coli*.

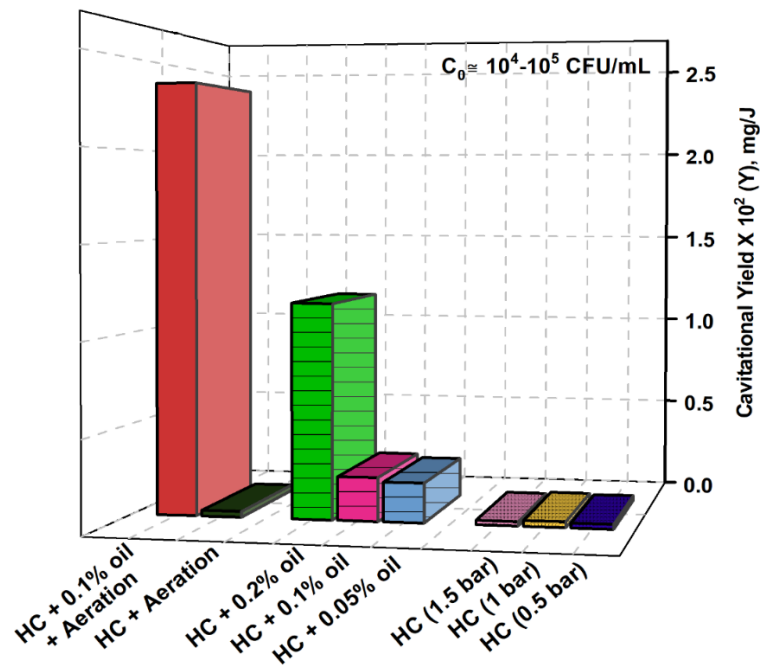


Fig. 9: Cavitation Yield

Table:

Table 1: Comparison of different processes

Processes	Disinfection (%)	Treatment Time (min)	$k \times 10^4$ (min ⁻¹)	Synergistic Index
Only AC	30	15	2.4	-
AC + 0.05% fennel oil	49	15	4.5	1.472
AC + 0.1% fennel oil	60	15	6.1	1.583
AC + 0.2% fennel oil	100	15	69.1	14.73
HC (ΔP 0.5 bar)				
Only HC (ΔP 0.5 bar)	59	60	1.8	-
HC + 0.1% fennel oil	91	60	5.0	1.541
HC + 0.2% fennel oil	100	2	664.5	128.5
HC (ΔP 1 bar)				
Only HC (ΔP 1 bar)	82	60	2.8	-
HC + 0.05% fennel oil	100	60	23.5	6.666
HC + 0.1% fennel oil	100	20	69.1	15.92
HC + 0.2% fennel oil	100	2	244.0	47.20
COMBINED PROCESS				
HC (ΔP 1 bar) + aeration	80	60	2.7	0.114
HC (ΔP 1 bar) + aeration+ 0.1% fennel oil	100	1	690.8	159.2

References

1. L. Armstrong, and E. Johnson, *Nutrients* 10, 1928, 2018.
2. M. Chaplin, *Biochem Mol Biol Educ.* 29, 54, 2001.
3. L. Yemi, *New Report on Inequalities in Access to Water, Sanitation and Hygiene Also Reveals More than Half of the World Does Not Have Access to Safe Sanitation Services.* 2019.
4. L. Hooper, N. Martin, A. Abdelhamid, and G. Davey Smith, *Cochrane Database Syst Rev*, 2015.
5. J.B. Kaper, J.P. Nataro, and H.L.T. Mobley, *Nat Rev Microbiol*, 2, 123, 2004.
6. V. Tyagi, A. Chopra, Kazmi A.A., and A. Kumar, *Iranian J Environ Health Sci Eng*, 3, 205, 2006.
7. S.T. Odonkor, and J.K. Ampofo, *Microbiol Res*, 4, 2, 2013.
8. D. Ghernaout, A.S. Alghamdi, and B. Ghernaout, *Applied Engineering*, 3, 13, 2019.
9. M. Lindmark, K. Cherukumilli, Y.S. Crider, P. Marcenac, M. Lozier, L. Voth-Gaeddert, D.S. Lantagne, J.R. Mihelcic, Q.M. Zhang, C. Just, and A.J. Pickering, *Environ Sci Technol*, 56, 9164, 2022.
10. M. Garvey, J. Hayes, E. Clifford, and N. Rowan, *Water Environ. J.*, 29, 27, 2015.
11. B.A. Younis, L. Mahoney, and N. Palomo, *Water*, 10, 1275, 2018.
12. K. Song, M. Mohseni, and F. Taghipour, *Water Res*, 94, 341, 2016.
13. S. S. Raj, Pooja Thanekar, Kshama Balapure, and V. M. Bhandari, *J. ISAS*, 2, 23, 2024.
14. K.K. Jyoti, and A.B. Pandit, *Biochem. Eng. J.*, 7, 201, 2001.
15. K.K. Jyoti, and A.B. Pandit, *Ultrason Sonochem*, 10, 255, 2003.
16. K.K. Jyoti, and A.B. Pandit, *Biochem. Eng. J.*, 18, 9, 2004.
17. P. Thanekar, and P. Gogate, *Fluids*, 3, 98, 2018.
18. M.B. Mane, V.M. Bhandari, and V. V. Ranade, *J. Water Proc. engineering*, 43, 2021.
19. M.B. Mane, V.M. Bhandari, K. Balapure, and V. V. Ranade, *Ultrason Sonochem*, 69, 2020.
20. N.B. Suryawanshi, V.M. Bhandari, L.G. Sorokhaibam, and V. V. Ranade, *Sci Rep*, 6, 2016.
21. P.G. Suryawanshi, V.M. Bhandari, L.G. Sorokhaibam, J.P. Ruparelia, and V. V. Ranade, *Environ. Prog. Sustain. Energy*, 37, 295, 2018.
22. K. Sharma, M. Chethana, V. Bhandari, L.G. Sorokhaibam, V. Ranade, and D. Killedar, *J. ISAS*, 1, 49, 2023.

23. V. V. Ranade, and V.M. Bhandari, *Industrial Wastewater Treatment, Recycling and Reuse*, Elsevier, 06975, 2014.
24. P. Jain, V.M. Bhandari, K. Balapure, J. Jena, V. V. Ranade, and D.J. Killedar, *J. Environ. Manag.*, 242, 210, 2019.
25. M.B. Mane, V.M. Bhandari, K. Balapure, and V. V. Ranade, *Ultrason Sonochem*, 61, 105272, 2020.
26. D. Dixit, V.M. Bhandari, M.B. Mane, and K. Balapure, *Biochem. Eng. J.*, 187, 108631, 2022.
27. K. Balapure, and V. Bhandari, *J. ISAS*, 2, 18, 2024.
28. W.R. Diao, Q.P. Hu, H. Zhang, and J.G. Xu, *Food Control*, 35, 109, 2014.
29. A.A. Shahat, A.Y. Ibrahim, S.F. Hendawy, E.A. Omer, F.M. Hammouda, F.H. Abdel-Rahman, and M.A. Saleh, *Molecules*, 16, 1366, 2011.
30. C.D. Köhler, and U. Dobrindt, *Int J. Med. Microbiol*, 301, 642, 2011.
31. P. Pokharel, S. Dhakal, and C.M. Dozois, *Microorganisms* 11, 344, 2023.
32. A. Leimbach, J. Hacker, and U. Dobrindt, *Curr. Top. Microbiol. Immunol.*, 358, 3, 2013.
33. V. V. Ranade, A.A. Kulkarni, and V.M. Bhandari, WO 2013054362, US9422952B2, 2013.
34. F. Anwar, M. Ali, A.I. Hussain, and M. Shahid, *Flavour Fragr. J.*, 24, 170, 2009.
35. W.R. Diao, Q.P. Hu, H. Zhang, and J.G. Xu, *Food Control*, 35, 109, 2014.
36. A. Mutlu-Ingok, G. Catalkaya, E. Capanoglu, and F. Karbancioglu-Guler, *Food Front* 2, 508, 2021.
37. R. Amorati, M.C. Foti, and L. Valgimigli, *J. Agric. Food Chem.*, 61, 10835, 2013.